LAPPEENRANTA UNIVERSITY OF TECHNOLOGY
FACULTY OF TECHNOLOGY
Master's Degree Programme in Technomathematics and Technical Physics

DEVELOPMENT OF PHASE RETRIEVAL ALGORITHM AND TECHNIQUES FOR OPTICAL SPECTRUM ANALYSIS

Examiners: Professor, Erik Vartiainen
Professor, Erkki Lähderanta

Supervisor: Professor, Erik Vartiainen

Lappeenranta 22.05.2008

Alexander Kolychev
Ruskonlahdenkatu 13-15 A1
53850 Lappeenranta
Phone: +358468932527

ABSTRACT

LAPPEENRANTA UNIVERSITY OF TECHNOLOGY
FACULTY OF TECHNOLOGY
Master's Degree Programme in Technomathematics and Technical Physics

Author: Alexander Kolychev

Title: **Development of phase retrieval algorithm and techniques for optical spectrum analysis**

Master's thesis

Year: 2008

65 pages and 31 figures.

Examiners: Professor, Erik Vartiainen,
Professor, Erkki Lähderanta.

Keywords: CARS, coherent anti-Stokes Raman spectroscopy, MEM, wavelets.

Coherent anti-Stokes Raman scattering is the powerful method of laser spectroscopy in which significant successes are achieved. However, the non-linear nature of CARS complicates the analysis of the received spectra. The objective of this thesis is to develop a new phase retrieval algorithm for CARS. It utilizes the maximum entropy method and the new wavelet approach for spectroscopic background correction of a phase function. The method was developed to be easily automated and used on a large number of spectra of different substances.. The algorithm was successfully tested on experimental data.

ACKNOWLEDGEMENTS

I wish to express my sincere thanks to Professor Erik Vartiainen for providing me an interesting research topic and for supervising me during preparation of this Thesis.

I wish to express my gratitude to Professor Erkki Lähderanta for his support and guidance during all my studies in Lappeenranta University of Technology and living in Lappeenranta.

Special thanks go to my parents for their support and encouragement to my work.

Lappeenranta, May 2008
Alexander Kolychev.

TABLE OF CONTENTS

SYMBOLS

Roman letters

A	MEM amplitude
c	approximation wavelet coefficient or variable
d	detail wavelet coefficient
E	electric field [V/m]
f	function or approximation component
G	highpass wavelet filter
g	detail component
H	lowpass wavelet filter
K	squeezing parameter
L	space
l	wavelet decomposition level
$\boldsymbol{k}$	wave vector [1/m]
M	number of autocorrelation coefficients
N	number of samples
P	dipole moment [C]
t	time [s]
R	all real axis
S	spectral line shape
W	energy [joule]

Greek letters

α, β	MEM coefficients
Γ	line width
ε	dielectric permittivity
η	normal coordinate
θ	final phase function [rad/s]
ν	normalized frequency
φ	error phase function [rad]
χ	dielectric susceptibility
ψ	full phase function or wavelet function [rad]
Ω, ω	frequency [rad/s]

1 INTRODUCTION

1.1 Laser spectroscopy

Last two or three decades are characterized by the great modifications in methods of the spectral analysis of atoms and molecules. It is connected with the application of lasers. The dream of many generations of spectroscopists has come true: in their hands there was a new light source of the big potency possessing monochromatic radiation with a small divergence. It has allowed not only to increase sensitivity and to simplify experimental techniques of existed methods: the new area of researches has appeared, laying on a joint of quantum electronics engineering and optical spectroscopy. It was laser spectroscopy.

One of the methods of laser spectroscopy is the spectroscopy of Raman scattering of light [1]. The first experiments on observation of Raman scattering have been connected with huge experimental difficulties. It was owing to extremely small intensity of the useful scattered signal arising at excitation by spontaneous light sources. As a result long lasting many hours exposures were necessary to derive spectra. After occurrence of lasers there was a rebirth of Raman spectroscopy. Application of lasers has allowed to bypass many difficulties. Times of exposure necessary for filing of spectra have been reduced by some orders, geometrical schemes of experiments are simplified, conditions for carrying out of temperature and polarizable experiments, etc. are improved.

Many types of objects such as liquids, dielectrics, semiconductors and metals became accessible to research.

Singularities of appearance of Raman scattering are intensively studied last years. Researches have approached to a series of new appearances. To them concern:

1. Resonance RS
2. Stimulated RS
3. Giant RS

4. Hyper RS

5. Coherent anti-Stokes RS

Among the new methods of laser spectroscopy in which significant successes are achieved, it is necessary to name coherent anti-Stokes Raman scattering spectroscopy (CARS). The coherent scattering of light is a strongly non-linear optical effect which is a non-linear variety of Raman scattering of light.

Coherent character of scattering in CARS spectroscopy causes its some basic advantages in comparison with spontaneous Raman spectroscopy: very high powers of signals, a small divergence of the scattered radiation, elimination of noise connected with a luminescence of examples.

1.2 Motivation of study

However, the nonlinear nature of CARS spectroscopy complicates the analysis of the received spectra. It is caused by the fact that the line shape in CARS spectra considerably differs from the form of a line shape in spontaneous Raman spectra. In many practical applications, for example, at the analysis of complicated substances, a priori knowledge of the vibrational spectra of spontaneous Raman measurements of separate components is necessary for correct extraction of the information from CARS spectra. Additional data is required because the intensity of the scattered radiation in the coherent spectroscopy does not depend directly on concentration of separate components in a substance. Therefore transformation of CARS spectra to Raman scattering spectra is necessary. Difficulties arise at the analysis of samples with unknown content when spectra of separate components are not available.

Thus the problem in extraction of the information from coherent anti-Stokes Raman scattering without any prior knowledge of additional spectral data is actual. Some techniques are already developed. One of them will be explained in the literature overview. However, the existing methods require the individual analysis for spectra of various substances.

1.3 The purpose of the work

The purpose of this Thesis is the development of an algorithm which extracts information from CARS spectra, suitable for maximum wide range of various substances. The origin of this work is to investigate a possibility of using wavelet decomposition in spectroscopic background removal.

In this work it is necessary to solve the following problems:

1. To receive experimental measurements of coherent anti-Stokes scattering spectra of various substances and some Raman scattering spectra for comparison.

2. To study and to analyze the known methods of extraction of the information from CARS spectra

3. To develop a phase retrieval algorithm, suitable for automatic computer processing. The algorithm will include the new method of spectroscopic background removal from CARS spectra.

4. To test the algorithm on spectra of different substances and to make conclusions about a possibility of application of the algorithm.

2 GENERAL INFORMATION ABOUT CARS SPECTROMETRY

2.1 Spontaneous Raman scattering of light

Under an action of an exterior electromagnetic field the dipole moments are induced in a substance. These moments are connected with the distortion of an electronic cloud of atoms [2]. Thus, it is possible to use series expansion on strength of exterior electric field E:

$$P = \chi_1 \epsilon_0 E + \chi_2 \epsilon_0 E^2 + \chi_3 \epsilon_0 E^3 + \ldots , \quad (1)$$

where p is the induced dipole moment of an atom; ε_0 is the absolute permittivity of a medium; χ_1, χ_2, χ_3 are corresponding linear and non-linear susceptibilities.

Susceptibilities χ_i = χ_1, χ_2, χ_3, etc., in turn, depend on disposition of nucleuses. Therefore it is possible to use series expansion on normal coordinates η of oscillations of nucleuses:

$$\chi_i = \chi_i^{(0)} + \left(\frac{d\chi_i}{d\eta} \right)^{(0)} \eta + \left(\frac{d^2\chi_i}{d\eta^2} \right) \eta^2 + \ldots \quad (2)$$

We shall present electric field strength in complex form:

$$E = E_0 e^{-i\omega_0 t} \quad , (3)$$

where ω_0 is the frequency of initial electromagnetic radiation. The oscillations of nucleuses should happen under the harmonic law. Accordingly, it is possible to suppose that $\eta = \eta \cos \Omega_i t = (1/2)\eta_0 (e^{i\Omega_j t} + e^{i\Omega_j t})$, where Ω_j are corresponding frequencies of normal oscillations of molecules or crystalline lattices. Thus, we have the equation for the induced dipole moment:

$$p = \chi_1^{(0)} \epsilon_0 E_0 e^{-i\omega_0 t} + \frac{1}{2} \left(\frac{d\chi_1}{d\eta} \right)^{(0)} \epsilon_0 E_0 \eta_0 [e^{-i(\omega_0 - \Omega_j)t} + e^{i(\omega_0 - \Omega_j)t}] + \chi_2^{(0)} \epsilon_0 E_0^2 e^{-i2\omega_0 t} +$$

$$+\frac{1}{2}\left(\frac{d\chi_1}{d\eta}\right)^{(0)}\epsilon_0 E_0^2\eta_0[e^{-i(2\omega_0-\Omega_j)t}+e^{-i(2\omega_0+\Omega_j)t}]. \quad (4)$$

Only the lowest factors of expansion on exterior field E and normal coordinate η are considered in the ratio (4). According to the common theory of radiation, the oscillating dipole moment leads to appearance of radiation which frequency is equal to the frequency of an oscillation of this dipole moment. The augend corresponds to the scattering of light without modification of frequency (Rayleigh scattering). The addend is caused by the Raman scattering, which happens due to modulation of an exterior field by optical oscillations with frequencies Ω_j. The third item is caused by the scattering of light, accompanied doubling of frequency ($\omega' = 2\omega_0$). It is called Hyper-Rayleigh scattering of light. The fourth item is caused by scattering on frequencies $\omega' = 2\omega_0 \pm\Omega_j$.

Thus, in a spectrum of light scattered by molecules of a medium, it is discovered not only a spectral line of a light source. There are also other lines which have the frequencies displaced in comparison with the exciting mode. These lines are Raman scattering modes. Scattering with smaller frequency $\omega - \Omega_j$ refers to Stokes, and with greater $\omega + \Omega_j$ refers to anti-Stokes scattering [2].

The basic experimental difficulties arising at registering of spontaneous Raman spectra are connected with very small intensity of the scattered radiation. Intensity of the strongest spontaneous lines makes only 10^{-6}—10^{-5} from the intensity of an exciting line. Weak lines can have intensity on some orders less. Besides the scattered light is radiated in a solid angle 4π steradian that leads to significant losses at its registration [3].

2.2 Coherent anti-Stokes Raman scattering of light (CARS)

Spontaneous Raman scattering of light is connected with thermal oscillations of molecules. It is a corollary of violation of a principle of superposition. Light waves and oscillations of a medium produce mutual influence against each other [4]. Raman spectroscopy studies the modulation of light by thermal (spontaneous) oscillations of molecules. It would be natural to expect a boomerang effect of action of light waves on molecular oscillations.

The reason of inverse action of the light waves on molecular oscillations is dependency $\chi(\eta_i)$. When a molecule gains a dipole moment in a field of a light wave, it starts to co-operate with the wave. The energy of this interaction is

$$W = -PE = -\chi(\eta_i)E^2. \quad (5)$$

Thus the force starts to act on the molecule:

$$F = \frac{-dW}{d\eta_i} = \frac{d\chi}{d\eta_i}E^2. \quad (6)$$

If two light waves (E_1 and E_2) are spread simultaneously in a medium and they have frequencies ω_1 and ω_2, then the field $E = E_1 + E_2$ and the force F will contain, in particular, a component varying with frequency $\omega_1 - \omega_2$. Usually waves E_1 and E_2 are the waves of visible range. Nevertheless it is possible to make the difference $\omega_1 - \omega_2$ very small, and in particular close to the frequency of normal oscillation: $\omega_1 - \omega_2 = \Omega_j$. The resonance swing of oscillations of atoms in molecules is possible in that case. In these conditions regular forced oscillations are superimposed on random molecular movement. The phases of these forced oscillations in various molecules are determined by phases of forcing fields E_1 and E_2. Having directed to such medium a probe wave with frequency ω, it is possible to observe Stokes and anti-Stokes waves with frequencies

$$\omega_{s,a} = \omega \pm (\omega_1 - \omega_2). \quad (7)$$

Effectiveness of energy exchange between interacting waves, as at any resonance, depends on phase relations between them. Therefore the scattered wave will have the greatest intensity in the certain directions along which phase relations between spread waves are kept. These directions are set by conditions of phase synchronism:

$$\boldsymbol{k}_{s,a} = \boldsymbol{k} \mp (\boldsymbol{k}_1 - \boldsymbol{k}_2). \quad (8)$$

$\boldsymbol{k}_{s,a}$ is the wave vector of Stokes and anti-Stokes waves, $\boldsymbol{k}_1, \boldsymbol{k}_2, \boldsymbol{k}_3$ are the wave vectors of the probe wave and pump waves accordingly. A corollary of this is the narrow directness of the scattered wave that allows to collect the scattered radiation

almost completely and to direct it to a photodetector [3].

The anti-Stokes scattering is considered to be the most interesting, as in anti-Stokes area, for example, there is no luminescence of a sample. The energy diagram is shown in Figure 1 [5].

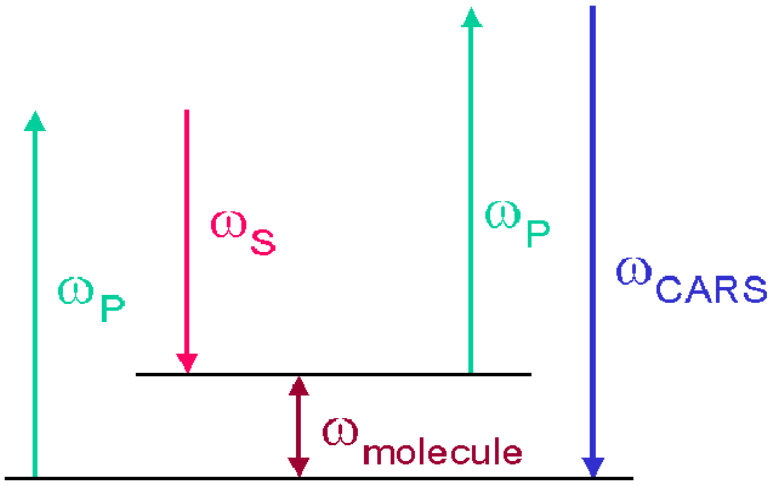

Figure 1. The energy scheme of CARS. ω_p is the frequency of a pump field, ω_s is the frequency of a Stokes field, $\omega_{molecule}$ is the frequency of natural oscillations of a molecule, ω_{CARS} is the frequency of a probe field [5].

It is natural, that scattering on the phase matching oscillations will lead to significant growth of intensity of the scattered light. It achieves 1% from intensity of the probe wave. It is necessary to underline, that so effective scattering is a corollary first of all phase matching or coherence of forced oscillations, instead of their big amplitude. The spectrum of a coherent scattering can be received, if there is a possibility of smooth frequency tuning of the pump waves.

The interesting singularity of the CARS signal is exhibited. Radiation, which is coherently scattered by molecules on frequency ω_a, consists of two components: the *resonant* component connected with oscillations of molecules, and the *non-resonant* component which is not connected with molecular oscillations. The second component practically does not depend on the difference in frequencies of the pump waves. As these components are coherent, they interfere among themselves and in a registered signal there are characteristic maxima and minima of intensity at scanning

the difference in frequencies near to frequency of a molecular resonance. Therefore the form of the line shape of molecular oscillations in spectroscopy CARS strongly differs from the form of a spontaneous Raman spectroscopy line [6].

2.3 Main principles and scheme of CARS spectrometry

The schematic diagram of experiments in CARS spectroscopy is presented in Figure 2. Two pulse lasers 1 and 2 create simple harmonic pump waves with frequencies ω_1 and ω_2. Frequency of radiation of the laser 2 is smoothly tuned. Radiation of lasers is focused by lenses 3 and 4 on a sample 5. Coherently scattered radiation on frequency ω_a is gathered by the lens 6 and goes in a monochromator 7. Intensity of the scattered radiation is registered by a photodetector 8. The common CARS spectrum is also presented in Figure 2. Non-scattered part of pump radiation is cut off by opaque screens 9 and 10. One of pump waves appears as a probe wave in this scheme. The angle between pump waves (for liquid samples it is 1°–3°) is taken such that the condition of phase synchronism is satisfied [3].

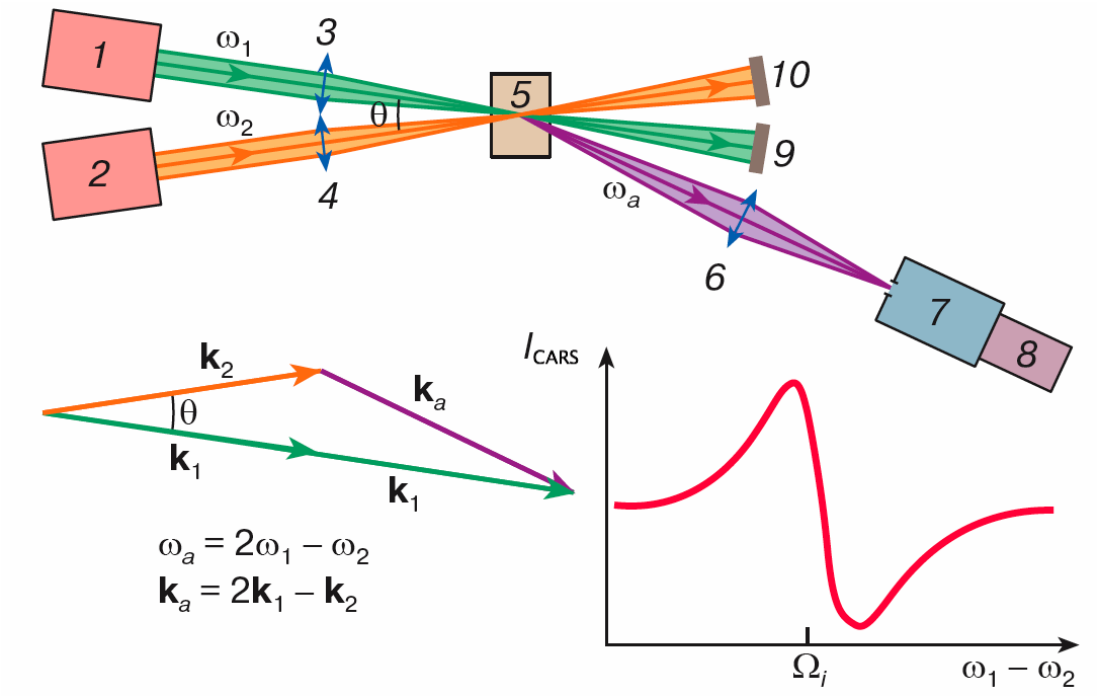

Figure 2. Schematic diagram of CARS spectrometer [3].

For investigation of fluid and solid samples the spectrometer on the basis of two pulse lasers creating emission on wave lengths λ_1 = 532 nm and λ_2 = 550 - 615 nm, with the pulse-recurrence frequency from tens Hz up to kHz and duration of an impulse about 10 ns and power 10 - 200 kW, can be used [3].

2.4 The advantages of CARS

The main advantages of CARS are [2,3,5,6]:

1. The small divergence of coherently scattered radiation allows to study shone plants: flames, discharges, etc. The solid angle of gathering of coherently scattered light is so small, that the contribution of a shone background noise becomes insignificant. Besides, the small area of overlapping of pump waves in a sample (microlitres) allows to study distribution of temperature and concentration of various gases in processes of combustion and plasma. CARS spectroscopy has found application for study of the processes happening in internal combustion engines (including jet and rocket drives), in turbulent gas jets, supersonic aerodynamic streams, etc.

2. High sensitivity of the method (which is proved in [7]), a possibility to use impulse lasers with small time of a pulse (nano-, picoseconds and less) make CARS spectroscopy a perspective method of research of fast relaxation processes, short-lived excited states, yields of photochemical responses, etc.

3. Unique possibilities of CARS spectroscopy are especially interesting to the analysis of complicated spectral contours under which some lines disappear.

Let's suppose, that in a researched sample there is a mixture of two grades of molecules. Some normal oscillation of molecules of the first grade has frequency Ω_1, and the second grade has Ω_2. If the difference $\Omega_1 - \Omega_2$ is great enough, the complicated contour which is presented in Figure 3(a) will be observed in the spectra of spontaneous Raman scattering. However if the frequencies of normal oscillations of these molecules differ slightly, we cannot judge how many and what components are hidden under it by the form the resulting contour 3 (b).

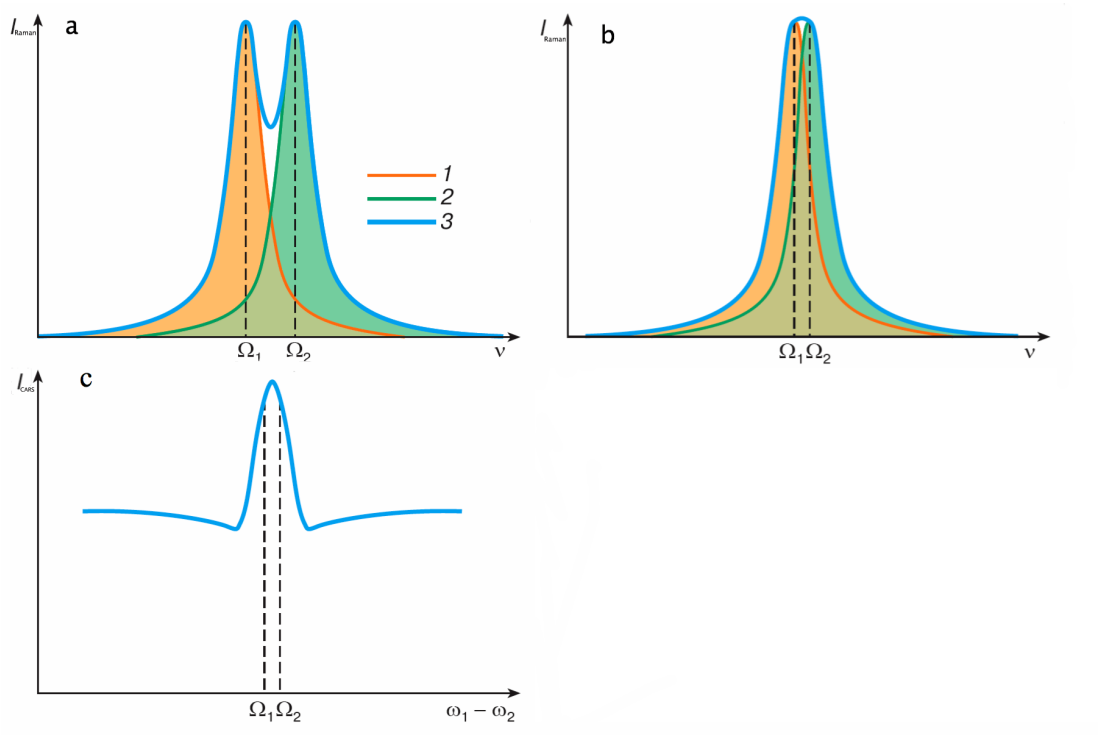

Figure 3. Interference in CARS spectra [3].

In essence, other picture is observed in CARS spectra. As the waves scattered by molecules of different grades are coherent, there will be their interference, instead of simple addition of the intensities as it happens in spontaneous Raman. The registered spectrum will represent result of an interference of three components of the scattered radiation: non-resonant background noise and the resonant radiation scattered on molecules of the first and second grades. The characteristic aspect of such spectrum is represented in Figure 3(c) [3].

It is necessary to note one more important point. The nonresonant background noise and resonant components in the scattered radiation are linearly polarized. Plane orientations of the resonant components polarization depend on properties of dispersing molecules and will be generally various. If we locate a polarizer before the entering slot of the monochromator, waves will pass through it, which strengths are equal to projections of the strength vectors of these components $E^{(non\text{-}r)}$, $E^{(1)}$ and $E^{(2)}$. Rotating a polarizer, it is possible to change magnitude of these projections and the contribution of these or those component to a registered interference picture. In other words, in CARS spectroscopy there is an unique possibility to control the form of an observable spectrum due to the modification of the relative share of scattered

waves in an observable signal.

Thus, the fundamental difference of CARS spectra in front of spontaneous Raman spectra consists in the coherent nature of CARS spectra. Separate spectral components are summed at the level of dielectric susceptibility, which results interference in the final spectral distribution. As a result maxima can amplify or on the contrary be extinguished from each other. In usual spontaneous scattering spectral components are summed at the level of intensity, and the resulting distribution is the simple sum of separate resonances [8].

3. RETRIEVAL OF THE PHASE FUNCTION IN CARS SPECTROMETRY

3.1 Phase retrieval problem

In the work [8] it was explained, that for correct extraction of the information from CARS spectra, generally it is required to measure the spectrum of spontaneous Raman scattering and to reveal separate modes. It makes possible to perform a least-squares fit of the theoretical expression of the CARS spectra to the experimental data. The required parameters can be usually deduced directly from the data.

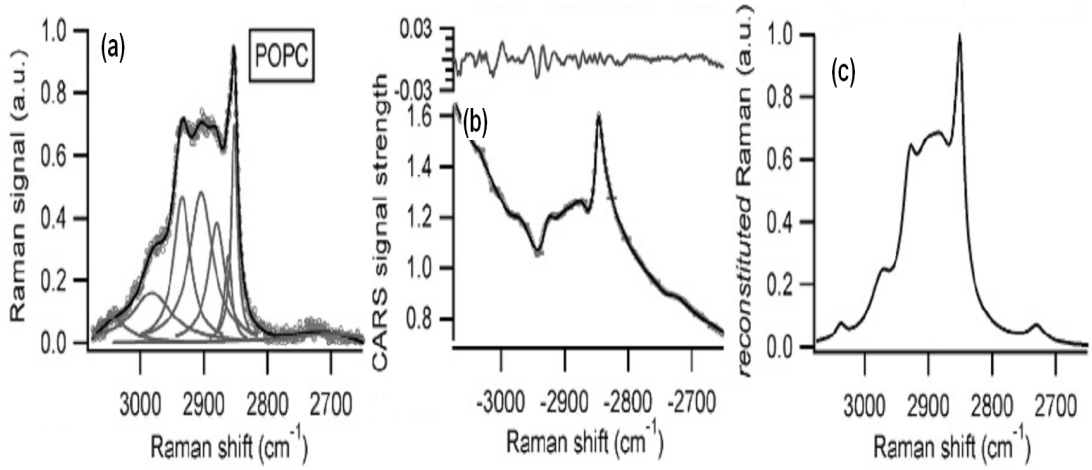

Figure 4. (a) is the spectrum of spontaneous Raman scattering, (b) is the CARS spectrum, (c) is the reconstituted spectrum a spectrum spontaneous Raman [9].

As an example in Figure 4 spectra of substance (1-Palmitoyl-2-oleoyl-sn-glycero-3-phosphocholine) (analyzed in the article [9]) are presented. In the first Figure 4(a) the spectrum of spontaneous Raman scattering is shown. Solid line represents the least-square fit to the experimental data using nine vibrational modes. In the second figure the spectrum of the same substance measured at the same temperature by CARS method is presented. In the second Figure 4(b) the measured CARS spectrum and its least-squares fit using the same nine vibrational modes are presented. If we try to calculate a reconstituted Raman spectrum from this least-squares fit, we will discover that it provides us with incomplete or incorrect information about the original

spectrum (Figure 4(c)).

As a result, following statements were suggested in [8]. It is possible to achieve a good fit for a spontaneous Raman spectrum by increasing the number of vibrational modes. But this is not true for a CARS spectrum. This is because of the fundamental difference between CARS and Raman spectra described above. Different spectral components in a CARS spectrum cause interference in a final spectrum, but for Raman it is just a sum of resonances.

The possibility of direct extraction of the Raman line shape from CARS spectra was demonstrated [8, 10]. It utilizes the maximum entropy method and does not require any prior knowledge of the vibrational resonances in a medium.

3.2 The maximum entropy method (MEM) in phase retrieval

The ideas of using MEM were completely described in the articles [8,10,14]. It is important for the following discussion to present the main results of these works.

Coherent anti-Stokes Raman scattering of light is a non-linear third-order optical process [3,4,11]. CARS signal is emitted owing to the third-order polarization $P^{(3)}(\omega_{as})$ which is produced by three fields. They are an electric pump field $E_{pu}(\omega_{pu})$, a Stokes field $E_s(\omega_s)$ and a probe field $E_{pr}(\omega_s)$. A femtosecond broadband laser is used in a multiplex CARS measurement. The Stokes field is produced by this laser. Both pump and probe fields are obtained from the same narrow-band laser. If we make all these fields parallel-polarized the CARS signal will be given by the equation [8,10]:

$$I_{CARS}(\omega_{as}) \propto |P^{(3)}(\omega_{as})|^2 = |E_{pu}|^2 |E_{pr}|^2 |E_s|^2 |\chi^{(3)}_{11111}(-\omega_{as}; \omega_{pu}, -\omega_s, \omega_{pr})|^2 \quad (9)$$

Where $\chi^{(3)}_{11111}$ is the corresponding component of the tensor of the nonlinear third-order dielectric susceptibility. As it was described above, a CARS spectrum consists of two parts. Thus, it is possible to consider $\chi^{(3)}_{11111}$ as the sum of non-resonant $\chi^{(3)}_{NR}$ and resonant Raman $\chi^{(3)}_{R}$ parts [12].

$$\chi^{(3)}_{1111}(\omega_{as}) = \chi^{(3)}_{NR} + \chi^{(3)}_{R} \quad , (10)$$

Where the non-resonant component is purely real and does not depend on frequency.

The resonant component is a complex function. It can be written as [12]:

$$\chi_R^{(3)} = \sum_j \frac{A_j}{\Omega_j - (\omega_{pu} - \omega_s) - i\Gamma_j} \quad (11)$$

Where A_j, Γ_j and Ω_j are the amplitude, the line width and the frequency of jth Raman mode accordingly. At experimental measurements the received CARS signal is normalized using reference signal from the sample which does not have vibrational resonances in the considered frequency range.

Thus, received spectral line shape $S(\omega_{AS})$ is proportional to the squared modulus $\chi_{1111}^{(3)}$:

$$S(\omega_{AS}) = \frac{|\chi_{NR}^{(3)} + \chi_R^{(3)}(\omega_{as})|^2}{|\chi_{NR,ref.}^{(3)}|^2} = |\chi_{nr}^{(3)} + \chi_r^{(3)}(\omega_{as})|^2 =$$

$$= \left(\chi_{nr}^{(3)}\right)^2 + 2\,\chi_{nr}^{(3)}\,\mathrm{Re}\left[\chi_r^{(3)}(\omega_{as})\right] + |\chi_r^{(3)}(\omega_{as})|^2. \quad (12)$$

Where $\chi_{nr}^{(3)}$ is the normalized non-resonant background term and $\chi_r^{(3)}$ is the normalized resonant Raman term [8,10,12].

For the purpose of extraction of the quantitative information from CARS spectra, for example, concentration of substance in a sample, the knowledge of imaginary component or phase function $\chi_r^{(3)}$ is necessary.

The spectral line of spontaneous Raman can be received from imaginary component of a linear dielectric susceptibility [8, 10]:

$$I_R \propto \sum_j |\chi_R^{(1)}(\omega)| = \sum_j \frac{A_j \Gamma_j}{(\Omega_j - \omega)^2 + \Gamma_j^2} \quad (13)$$

From comparison of expressions (11) and (13) it is visible, that imaginary components $\chi_R^{(3)}$ in CARS spectra and $\chi_R^{(1)}$ in spontaneous Raman spectra contain the identical spectral information and they can be compared. The

determination of phase function of a CARS spectrum allows to reconstitute the spontaneous Raman line shape. For a determination of phase function the maximum entropy method is used as the most optimum. Application of MEM in CARS is described in the works [8,10, 13, 14]

A typical CARS spectrum consists of approximately 250 points, spaced by 2,6 cm^{-1}. They cover a spectral range about 650 cm^{-1} [8].

The basic equation for the maximum entropy model for a CARS line shape [13]:

$$S(\nu;K)=\left|\frac{\beta(K)}{1+\sum_{p=1}^{M}a_p(K)\exp(-2\pi p\nu)}\right|^2=\left|\frac{\beta(K)}{A_M(\nu;K)}\right|^2 \quad (14)$$

Here the spectrum is decomposed into M Fourier components A_M. Each component can be expresses as:

$$A_M(\nu;K)=1+\sum_{p=1}^{M}a_p(K)\exp(-2\pi p\nu)=|A_M(\nu;K)|\exp[i\psi(\nu;K)] \quad (15)$$

Where ν is the normalized frequency from the least and greatest frequencies in a CARS spectrum and squeezing parameter K.

$$\nu=\frac{1}{2K+1}\left(\frac{\omega_{as}-\omega_{min}}{\omega_{max}-\omega_{min}}+K\right);\ \omega_{min}\le\omega\le\omega_{max};\ K=0,1,... \quad (16)$$

Special interest is represented with a phase since it contains the information necessary for converting of a CARS spectrum to spontaneous Raman. It can be presented as [10]

$$\psi(\nu,K)=\theta(\nu)-\phi(\nu,K) \quad (17)$$

Where $\phi(\nu,K)$ is the error phase, and $\theta(\nu)$ is the final phase function.

S (ν; K) corresponds with S (ω_{as}; K) as follows [8]:

$$S(\nu;K)=\begin{cases} S(\omega_{min});\ if\ 0<\nu<\dfrac{K}{2\mathrm{K}+1};\ \omega<\omega_{min} \\ S(\omega);\ if\ \dfrac{K}{2\mathrm{K}+1}<\nu<\dfrac{K+1}{2\mathrm{K}+1};\ \omega_{min}<\omega<\omega_{max} \\ S(\omega_{max});\ if\ \dfrac{K+1}{2\mathrm{K}+1}<\nu\le 1;\ \omega>\omega_{max} \end{cases} \quad (18)$$

Coefficients a_p and β in the equation of the MEM model (14) are received by solution of system of simple equations [13,14].

$$\begin{bmatrix} C(0) & C^*(1) & \cdots & C^*(M) \\ C(1) & C^*(0) & \cdots & C(M-1) \\ \vdots & \vdots & \ddots & \vdots \\ C(M) & C(M-1) & \cdots & C(0) \end{bmatrix} \begin{bmatrix} 1 \\ a_1 \\ \vdots \\ a_M \end{bmatrix} = \begin{bmatrix} |\beta|^2 \\ 0 \\ \vdots \\ 0 \end{bmatrix} \quad (19)$$

Where * means complex conjugate. Autocorrelation coefficients C(m) are defined by the discrete Fourier transform of a CARS line shape at the discrete set of normalized frequencies $\nu_n = n/N\ (n=0,1,\ldots,N)$. Thus,

$$C(m;K)=N^{-1}\sum_{n=0}^{N-1} S(\nu_n;K)\exp(2\pi i m\nu_n), \quad (20)$$

where $N=(2\mathrm{K}+1)(N_0-1)+1$ and $\mathrm{N_0}$ is the number of samples S (υ_N; K).

Thus, it is necessary to determine two parameters for the maximum entropy model: the number of autocorrelation coefficients *M + 1* and the value of the squeezing parameter K. Magnitude of M is limited by the number of data samples: $M \le N/2$. If we use the greatest possible value $M = M_{max}$, MEM approximates required phase function to the true one most precisely [8].

However by using the maximum value of M we transfer to phase function also noise from the initial spectrum. To reduce this noise we should reduce the magnitude of M. Best value M is taken so that it is large enough for a good approximation to the true function and small enough to remove parasite noise.

Squeezing parameter is easier to choose. It can be set to zero, then $S(\nu;K)=S(\omega_{as})$. However, if K > 0, $S(\omega_{as})$ is squeezed to narrower range.

It matters when using MEM for definition of the phase function. When the value of K is more than one, it leads to magnification of a constant background in the resulting phase . In practice in CARS spectroscopy only two values K=0 and K=1 are used.

It is important to note, that the phase function $\psi(\nu;K)$ has been received exclusively from approximation of the measured CARS spectrum by the maximum entropy method, i.e. directly from CARS measurements. As a result the error function $\phi(\nu;K)$ is the unique unknown part in the equation. Moreover, the function $\psi(\nu,K)$ and the function $\theta(\nu)$ contain the identical spectral information because the error function is non-resonant and is simply a background term.

Thus, there is a problem of definition of error function which represents a slowly varying background. In CARS spectroscopy the spectrum consists of very narrow resonance band arranged on the large background. Then in the elementary case it is possible to assume, that $\theta=0$ for the part of a spectrum where there are no strongly visible resonances [8,10].

$$\theta=\tan^{-1}\left[\frac{\operatorname{Im}\chi_r^{(3)}(\nu)}{\chi_r^{(3)}+\operatorname{Re}\chi_r^{(3)}(\nu)}\right]\approx 0 \quad (21)$$

Where lays far from all resonances. We receive

$$\theta_{est}(\nu)=\phi_{est}(\nu)+\psi(\nu;K)\approx\theta(\nu). \quad (22)$$

The required spontaneous line shape in that case is the equation:

$$\operatorname{Im}\left[\chi_r^{(3)}(\nu)\right]\approx\sqrt{S(\nu)}\sin\theta_{est}(\nu). \quad (23)$$

That is the first way of background correction.

3.3 The problem of the background term

The example of calculation of a spectrum by the above described method is presented in Figure 5.

MEM has been utilized on the measured CARS spectrum 5(a). The phase ψ 5(b) had been received. Background term (dashed line) was calculated approximately. In Figure 5(c) the spectrum received by application of MEM ($\mathrm{Im}\{\chi^{(3)}\}$) is shown in comparison with spontaneous Raman spectrum measured directly ($\mathrm{Im}\{\chi^{(1)}\}$) [10].

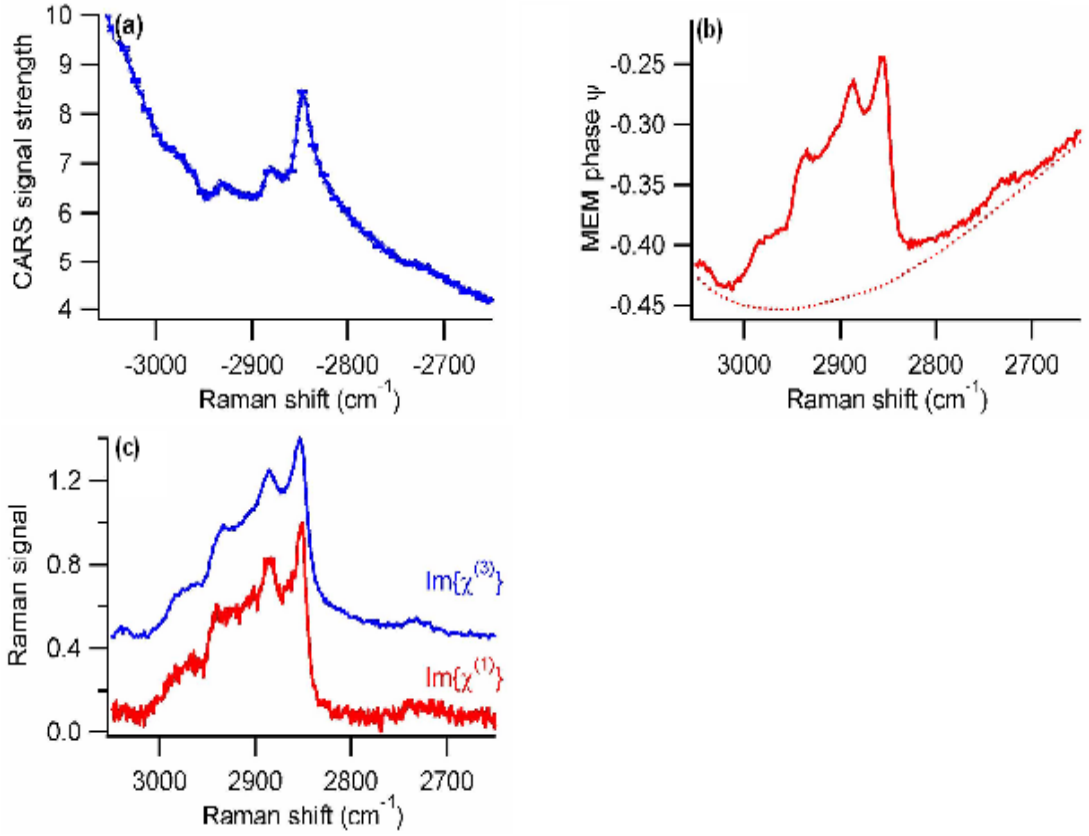

Figure 5. The maximum entropy method [10].

In this case the background term of the phase was obtained by guessing those part of the spectrum where the resonance is observed. Such method is difficult to program on a computer language. The main problem of the given work is to develop an algorithm which could be programmed easily.

4 WAVELETS

4.1 Introduction to wavelets

The wavelet analysis represents a special type of linear transform of signals and physical data represented by these signals about processes and physical properties of mediums and objects. The basis of the eigenfunctions, on which expansion of signals is spent, possesses many special properties and possibilities. They allow to concentrate attention to those or other singularities of analyzed processes which cannot be revealed by means of traditional Fourier and Laplace transforms.

Wavelets are the functions of a definite form localized on the axis of arguments (explanatory variables), invariant to shift and linear to operation of scaling (compression/stretching). They form by means of special basis functions which determine their aspect and properties. On localization in temporary and frequency representation wavelets occupy the intermediate position between the harmonic functions localized on frequency, and the function of Dirac localized in time. For the first time this term was used by A. Grossmann and J.Morlet at the analysis of properties of seismic and acoustic signals [15].

The theory of wavelets is not the fundamental physical theory, but it gives the convenient tool for a solution of many practical problems. The basic scope of wavelet transforms is the analysis and processing of signals and functions which are non-stationary in time or inhomogeneous in space, when outcomes of the analysis should contain not only common frequency characteristics of a signal, but also information about the certain local coordinates. In comparison with Fourier series expansion of signals, wavelets are capable with much higher exactitude to represent local singularities of signals. Unlike transforms of Fourier, the wavelet transform of one-dimensional signals ensures two-dimensional result, thus frequency and coordinate are considered as explanatory variables that enables the analysis of signals at once in two spaces.

One of the principals of wavelet representation of signals at various levels of decomposition consists in separation of functions of an approximation to a signal on two groups: approximation group, which is rough, with enough slow temporary

dynamics of modifications, and detail group, which has local and fast dynamics of modifications on a hum noise of smooth dynamics. It is possible both in temporary, and in frequency areas of wavelet representation of signals.

Integral Fourier transform and Fourier serieses are the basis of the Fourier analysis. Fourier coefficients received as a result of the transform, give in enough information for simple physical interpretation, and simplicity at all does not belittle importance of the subsequent conclusions about character of an investigated signal. Application of the integral Fourier transform and Fourier serieses (in evaluations, analytical transforms) is very obvious, all necessary properties and formulas leave by means of only two real-valued functions sin*(t)*, cos*(t)* (or one complex which is a sine wave $\cos(it)=\cos(t)+i\sin(t)$) [15].

4.2 Basic wavelet theory

Wavelet transform is not so good and widely known as Fourier, as it is applied rather recently and is in a stage of active development. We shall briefly describe the bases of wavelet transforms (mainly from the article [16]).

$L^2(R)$ is the space of the functions $f(t)$ on the all real axis $R(-\infty,\infty)$. This space has the definition of norm:

$$E_f=\int_0^{2\pi}|f(t)|^2dt=\sum_{-\infty}^{\infty}|c_n|^2. \quad (24)$$

The spaces $L^2(0,2\pi)$, which is used in expansions of Fourier, and $L^2(R)$ are much different from each other. If we define the space on the all real axis $L^2(R)$, the average value of a function should aspire to zero on $\pm infinity$. The sine wave, in that case, does not belong to $L^2(R)$ space, and, hence, the set of sine waves cannot be the basis of this functional space. It is necessary to discover simple enough functions for designing basis of the space $L2(R)$.

The waves which form the space $L^2(R)$, should aspire to zero at $\pm\infty$ and for practical purposes the faster, the better. We shall use well localized solitary waves as the basis functions. They are wavelets.

All Fourier space $R^2(0,2\pi)$ is completely built up by means of only one basis function $w(t)$. In the case of wavelets, we will try to build the functional space $L^2(R)$ the same way. That is we use only one wavelet $\psi(t)$. We shall note, that it can be a wavelet with one frequency or with a gang of frequencies. Let's first describe discrete transforms.

The task is to cover all real axis $R(-\infty,\infty)$ using only one localized function which fast aspires zero. Most simply it can be made, having provided system of shifts or transpositions along an axis. Let for simplicity they will be integer values, i.e $\psi(t-k)$.

Now we need an analogue of a sine wave frequency. For simplicity we shall note it through degrees of the two: $\psi(2^j t-k)$, here j and k are integers. Thus, by means of discrete scale transforms ($1/2^j$) and shifts ($k/2^j$) we can describe all frequencies and cover all axis, having unique basis wavelet $\psi(t)$ [16].

Definition of norm:

$$\|p\|_2=\langle p,p\rangle^{1/2}, \quad (25)$$

$$\langle p,q\rangle=\int_{-\infty}^{\infty} p(t)q^*(t)dt \quad . (26)$$

Hence,

$$\|\psi(2^j t-k)\|_2=2^{-j/2}\|\psi(t)\|_{2,} \quad (27)$$

I.e. if a wavelet $\psi\in L^2(R)$ has unit norm, then all wavelets from the set of $\{\psi_{jk}\}$

$$\psi_{jk}(t)=2^{j/2}\psi(2^j t-k), j,k\in I \quad (28)$$

have also norm 1, i.e. $\|\psi_{jk}\|_2=\|\psi\|_2=1$.

Wavelet $\psi\in L^2(R)$ is called orthogonal if the set $\{\psi_{jk}\}$ defined by the expression (28) represents orthonormal basis of a function space $L^{(R)}$, i.e.

$$\langle \psi_{jk}, \psi_{\Im} \rangle = \delta_{jl} \delta_{km} \quad (29)$$

And each function $f \in L^2(R)$ could be presented in the form of the series

$$f(t) = \sum_{j,k=-\infty}^{\infty} c_{jk} \psi_{jk}(t). \quad (30)$$

A simple example of an orthogonal wavelet is HAAR-wavelet, named so after Haar who had suggested it. This wavelet is defined by the relations

$$\psi^H(t) = \begin{cases} 1, & 0 \le t < 1/2, \\ -1, & 1/2 \le t < 1, \\ 0, & t < 0, t \ge 1. \end{cases} \quad (31)$$

We shall construct basis of a function space $L^2(R)$ by means of continuous scale transforms and transpositions of the wavelet $\psi(t)$ with arbitrary values of basis parameters [16]. We shall use the scale factor *a* and the parameter of shift *b*:

$$\psi_{ab} = |a|^{-1/2} \psi\left(\frac{t-b}{a}\right), \quad a, b \in R, \quad \psi \in L^2(R) \quad (32)$$

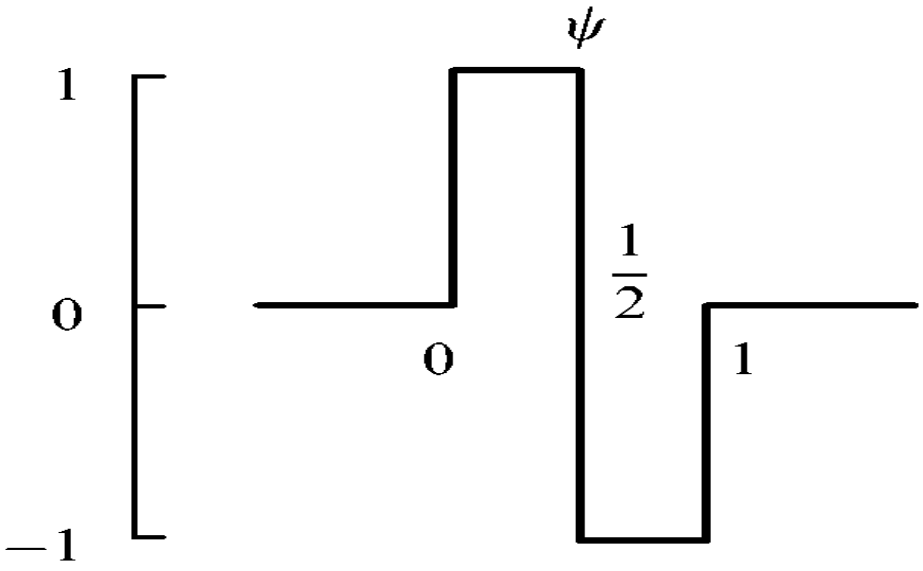

Figure 6. HAAR wavelet

Now we can write the integral wavelet transform on its basis [17]:

$$[W_\psi f](a,b)=|a|^{-1/2}\int_{-\infty}^{\infty} f(t)\psi^*\left(\frac{(t-b)}{a}\right)dt=\int_{-\infty}^{\infty} f(t)\psi^*_{ab}(t)\,dt \quad (33)$$

Let's spend the further analogy to Fourier transform. Coefficients c_{jk} of the wavelet series expansion (30) we can determine through the integral wavelet transform:

$$c_{jk}=[W_\psi f]\left(\frac{1}{2^j},\frac{k}{2^j}\right). \quad (34)$$

So, each function from the space $L^2(R)$ can be determined the sum of scale transforms and shifts of the basis wavelet, i.e. this is a composition of "wavelet waves".

Use of discrete wavelet transform allows us to lead the proof of many rules of the wavelet theory, connected with completeness and an orthogonality of basis, convergence of series, etc. It is necessary to prove this rules, for example, at compression of the information or in problems of numerical modeling.

Let's consider *inverse wavelet transform* [17]. The sine wave forms orthonormal basis of the function space $L^2(0,2\pi)$ and problems do not arise with inverse transform of Fourier. But in the wavelet transforms the basis $L^2(R)$ is not always orthonormal. It is defined by a choice basis wavelet, and a mode of construction of the basis (values of basis parameters *a*, *b*). However strict proofs of completeness and orthogonality are complicated. Besides for practical purposes it is enough to have "approximate" orthogonality of a system of expansion functions, i.e. that is enough, that it is "almost the basis".

Let's write out inverse transform for those two cases that are described above: for the basis (28) supposing expansions and shifts, and the basis (32) constructed at arbitrary values (*a*, *b*).

At the basis parameters (a,b), $a,b\in R$ inverse wavelet transform is written by means of the same basis, as the direct [16]:

$$f(t)=C_\psi^{-1}\int\int[W_\psi f](a,b)\psi_{ab}(t)\frac{da\,db}{a^2}, \quad (35)$$

C_ψ is the normalizing coefficient (similar to the coefficient which normalizes Fourier transform):

$$C_\psi = \int_{-\infty}^{\infty} |\hat{\psi}(\omega)|^2 |\omega|^{-1} d\omega < \infty \quad (36).$$

The condition of finiteness of the constant C limits the class of functions which can be used as a wavelet basis. In particular, it is obvious, that the Fourier imager should be equal to zero at the origin of coordinates and, hence, it should be equal to zero at least at zero moment: $\int_{-\infty}^{\infty} \psi(t) dt = 0.$

More often in applications that is enough reviewing only positive frequencies, i.e. $a > 0.$ Wavelet, accordingly, should satisfy to the condition

$$C_\psi = 2\int_{-\infty}^{\infty} |\hat{\psi}(\omega)|^2 |\omega|^{-1} d\omega = 2\int_{-\infty}^{\infty} |\hat{\psi}(-\omega)|^2 |\omega|^{-1} d\omega < \infty \quad (37)$$

In case of discrete wavelet transform the steady basis is defined as follows.

Function $\psi \in L^2(R)$ is called R-function if the basis $\{\psi_{jk}\},$ defined by expression (28), is the basis of Riesz in the sense that there are two constants A and $B,$ for which the relation

$$A\|\{c_{jk}\}\|_2^2 \le \left\| \sum_{j=-\infty}^{\infty} \sum_{k=-\infty}^{\infty} C_{jk} \psi_{jk} \right\|_2^2 \le B\|\{\} c_{jk}\|_2^2 \quad (38)$$

is true at any sequences $\{c_{jk}\}$:

$$\|\{c_{jk}\}\|_2^2 \le \sum_{j=-\infty}^{\infty} \sum_{k=-\infty}^{\infty} |C_{jk}|^2 < \infty. \quad (39)$$

For any R-function there is a basis $\{\psi^{jk}\},$ which is “double” of basis $\{\psi_{jk}\}$ by means of which it is possible to construct the reconstruction expression

$$f(t) = \sum_{j,k=-\infty}^{\infty} \langle f, \psi_{jk} \rangle \psi^{jk}(t). \quad (40)$$

If ψ is the orthogonal wavelet and $\{\psi_{jk}\}$ is the orthonormal basis then $\{\psi^{jk}\}$ and

$\{\psi_{jk}\}$ coincide and the formula is formula of inverse transform. If ψ is not orthogonal wavelet, but is two-place or conjugate R-wavelet, it has the double ψ by means of whom the double of a set $\{\psi_{jk}\}$ is constructed similarly to the basis [16]:

$$\psi^{jk}=\dot{\psi}^{*}_{jk}=2^{j/2}\psi(2^{jt}-k),\ j,k\in I. \quad (41)$$

4.3 Wavelet analysis applied to removing of a spectroscopic background

Spectroscopic background can be divided into two types: constant and varying. In the first case background correction does not represent difficulties since the background remains constant at various spectral measurements. However, in the second case, when spectroscopic background is not constant at various measurements, correction is a rather difficult task, especially if it should be made automatically.

Further the so-called algorithm of a "wavelet prism" (which is explained in the article [18]) is described. According to the theory of wavelets, the signal in the space $L^2(R)$ has unique wavelet representation, if certain conditions are met. The discrete signal f_i, for example, can be presented as

$$f_i=g_{i-1}+...+g_{i-l}+f_{i-l} \quad (42)$$

Where f_{i-l} is the approximation component, which frequency is no larger, than 2^{i-l}. This component is orthogonal to the detail components x_j at various levels $j(j=i-1,...,i-l)$. These detail components in turn are orthogonal among themselves and their frequencies are in a range from 2^{j+1} up to 2^j. Generally undesirable spectroscopic background is a low-frequency component of the signal. Thus, for a solution of the problem of background correction it is possible to use wavelet decomposition. It does not depend on the type of a background (constant or varying).

On the basis of the fast wavelet transform algorithm (Mallat algorithm [19]),

decomposition can be made by means of the linear mathematical operations using scaling function and wavelet orthogonal filters: a lowpass filter *H* and a highpass filter *G*.

We can write for the first linear transform:

$$\begin{cases} c_{i-1}^{1} = Hc_{i}^{0} \\ d_{i-1}^{1} = Gc_{i}^{0} \end{cases} \quad (43)$$

Thus, for the j[th] transform we have

$$\begin{cases} c^{j+1} = Hc^{j} \\ d^{j+1} = Gc^{j} \\ j = 0,1,\dots,l. \end{cases} \quad (44)$$

This decomposition can be presented as

$$\boxed{\begin{array}{c} c^{0} \to c^{1} \to c^{2} \to \dots c^{l-1} \to c^{l} \\ \searrow \quad \searrow \quad \searrow \quad \quad \searrow \\ d^{1} \quad d^{2} \quad d^{3} \quad \dots \; d^{l} \end{array}} \quad (45)$$

Low-frequency and high-frequency filters define approximation and detail coefficients. High-frequency coefficients have high resolution whereas low-frequency coefficients have low resolution. However, these two types do not give the information about the time resolution of the spectrum for deriving the information about spectroscopic background. The basic difficulty here consists in definition of a level of wavelet decomposition on which spectroscopic background is observed which is necessary for its removing [18] .

Generally reconstruction of an original spectroscopic signal can be lead by means of inverse linear wavelet transform:

$$c^{j} = H^{T} c^{j+1} + G^{T} d^{j+1}, \quad j = 0,1,\dots,l \quad (46)$$

Transform can be presented also as:

$$\begin{array}{ccccccccc} c^l & \rightarrow & c^{l-1} & \rightarrow & \ldots & c^2 & \rightarrow & c^1 & \rightarrow & c^0 \\ & \nearrow & & \nearrow & & & \nearrow & & \nearrow & \\ & d^1 & & d^{l-1} & & \ldots & & d^2 & & d^1 \end{array} \quad (47)$$

Wavelet inverse transform is a linear transformation, therefore it can be presented as the sum of terms:

$$f(=c^0) \approx g_1 + g_2 + \ldots + g_l + f_1 \quad (48)$$

Where:

$$\begin{aligned} g_1 &= G^T d^1 \\ g_2 &= H^T G^T d^2 \\ &\vdots \\ g_l &= \underbrace{H^T H^T \ldots H^T}_{l-1} G^T d^l \\ f_l &= \underbrace{H^T H^T \ldots H^T}_{l} c^l \end{aligned} \quad (49)$$

Approximation (f_1) and detail ($g_l, \ldots, g_2, g_1$) components are reconstructed directly from wavelet coefficients ($c^l, d^l, \ldots, d^2, d^1$). These components are orthogonal among themselves, create the contribution of various range of frequencies to a signal and have same resolution as the original signal. As shown in a Figure 7, the described wavelet transform splits a signal like a prism splits light waves. Such method is called method of "wavelet prism".

It is visible in the figure that the probable spectroscopic background can be found in the lowest frequencies (such as f_{10}). Noise components are found at high-frequency components (such as g_1, g_2).

Thus, the following two conclusions were made in the article [18]:

- The spectroscopic background is the spectral component arranged in low frequencies of wavelet decomposition (f_b), whereas the useful signal is located in middle frequencies (g_s). Noise is the third component of a spectrum, which is usually observed on the higher frequencies (g_n).

- Background, useful and noise components of a signal are not superimposed among themselves and submit to a rule of additivity

$$f = g_n + g_s + f_b \quad (50)$$

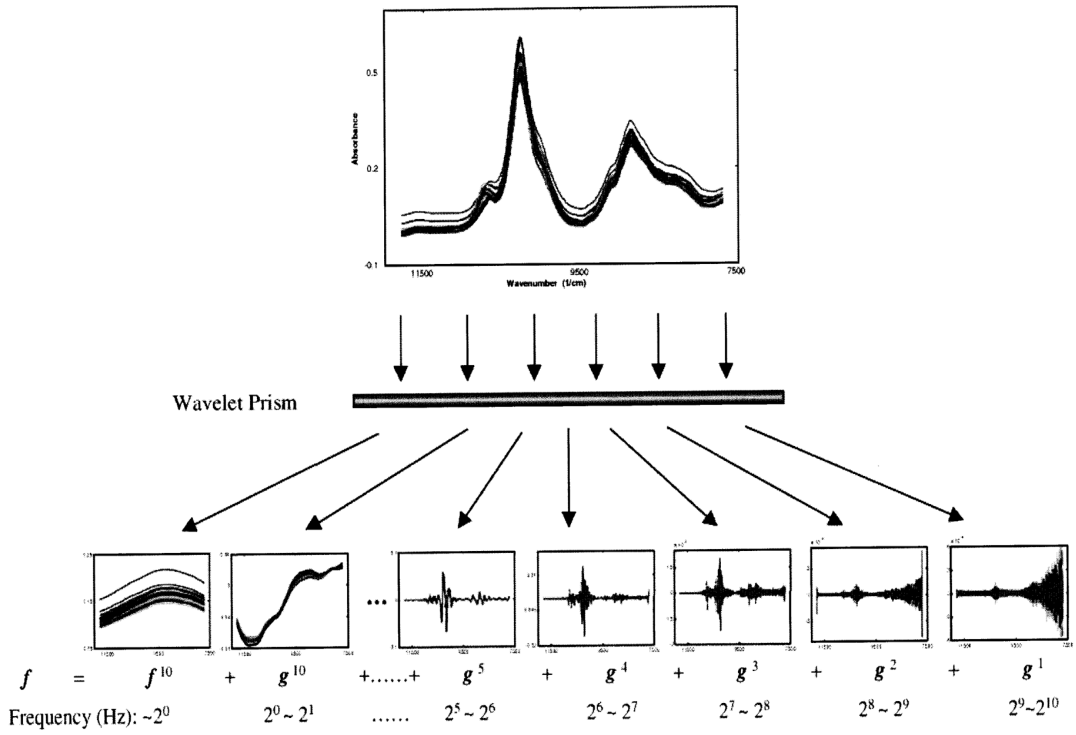

Figure 7. “Wavelet prism” principle [18].

Thus, there is a possibility to eliminate the last item in the expression (50), as it will be elimination of a spectroscopic background.

5 EXPERIMENTAL SECTION

5.1 Basic information about the spectrometers

To utilize all benefits of CARS spectrometry the multiplex CARS approach is used, which provides one with a signal with high signal-to-noise ratio.

CARS spectrometers are described in lots of works [20-24]. Let's briefly discuss the experimental setup for CARS measurements. Two lasers "Laser" and "Stokes" are synchronized on frequency and on time. They are focused by the objective of the microscope O_1 on an investigated sample. Scattered CARS signal is collected in the forward direction by the second objective O_2 and transited through the holographic filter F_1 and the short-wave filter F_2. Then the signal is collected by the spectrometer with CCD sensors.

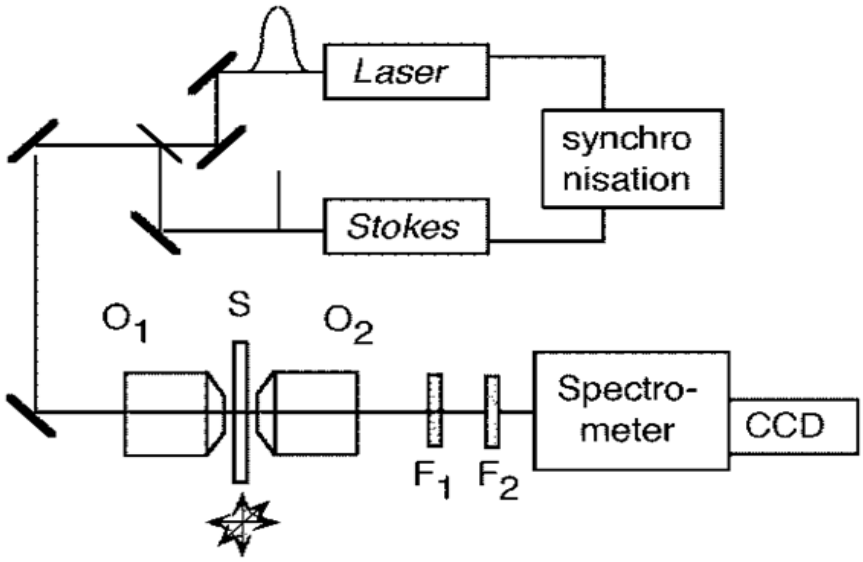

Figure 8. The scheme of the CARS spectrometer [22].

The pump laser generates 10 ps impulses with the central wave length 710 nm. The Stokes laser provides 80 fs impulses with the central wave length tunable between 750 and 950 nm that corresponds to the vibrational range 750 - 3500 cm^{-1}. Also this laser sets the sync for the second laser (works as a "master" laser).

Typical mean power on a sample is 95 and 25 mW for the pump laser and the Stokes laser accordingly.

A Raman microscope with 6 mW He-Ne laser was used for spontaneous Raman scattering measurements. It has spectral resolution 5 cm^{-1}.

5.2 Experimental data

The spectra of two samples were provided for the analysis: the DMPC (1,2-Dimyristoyl-sn-glycero-3-phosphocholine) lipid and the AMP/ADP/ATP mixture.

Measured CARS spectrum of AMP/ADP/ATP is presented in Figure 9. Spontaneous Raman spectrum of the same sample is shown in Figure 10.

CARS spectrum of the DMPC is presented in Figure 11.

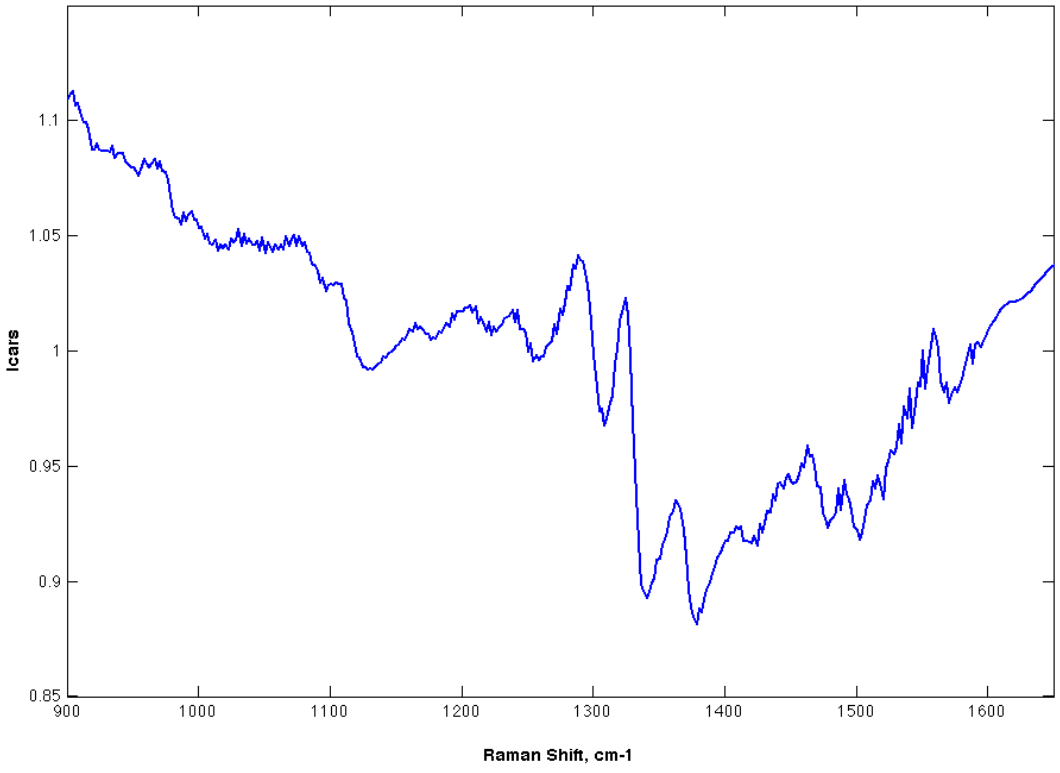

Figure 9. CARS spectrum of the AMP/ADP/ATP mixture

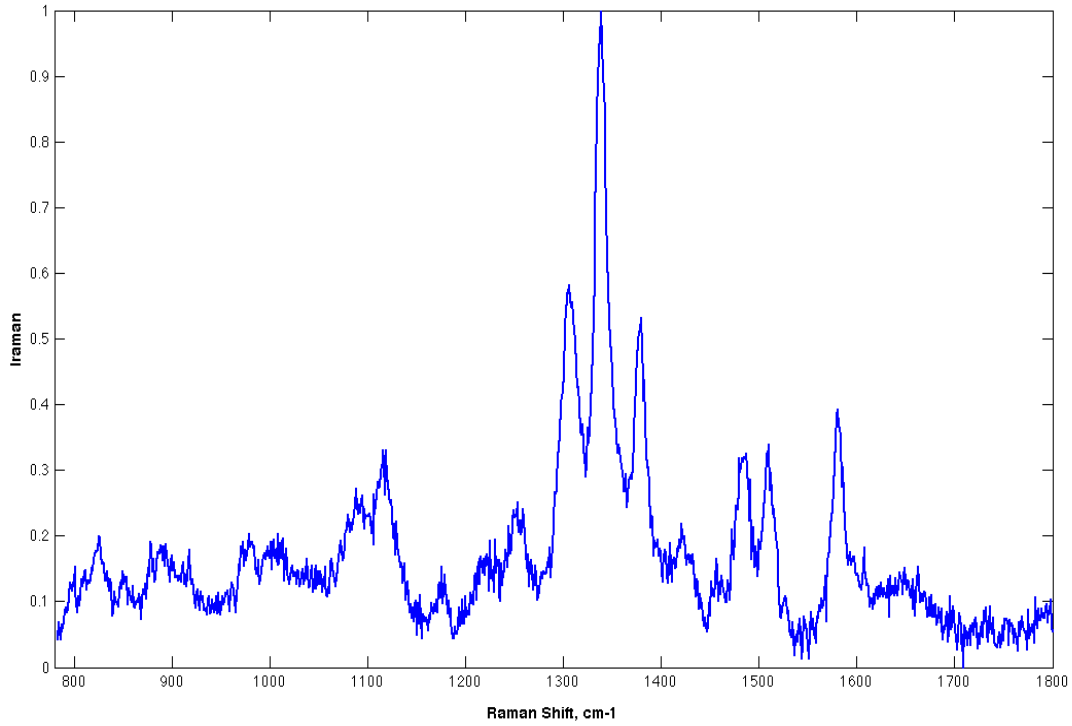

Figure 10. Spontaneous Raman spectrum of the AMP/ADP/ATP mixture

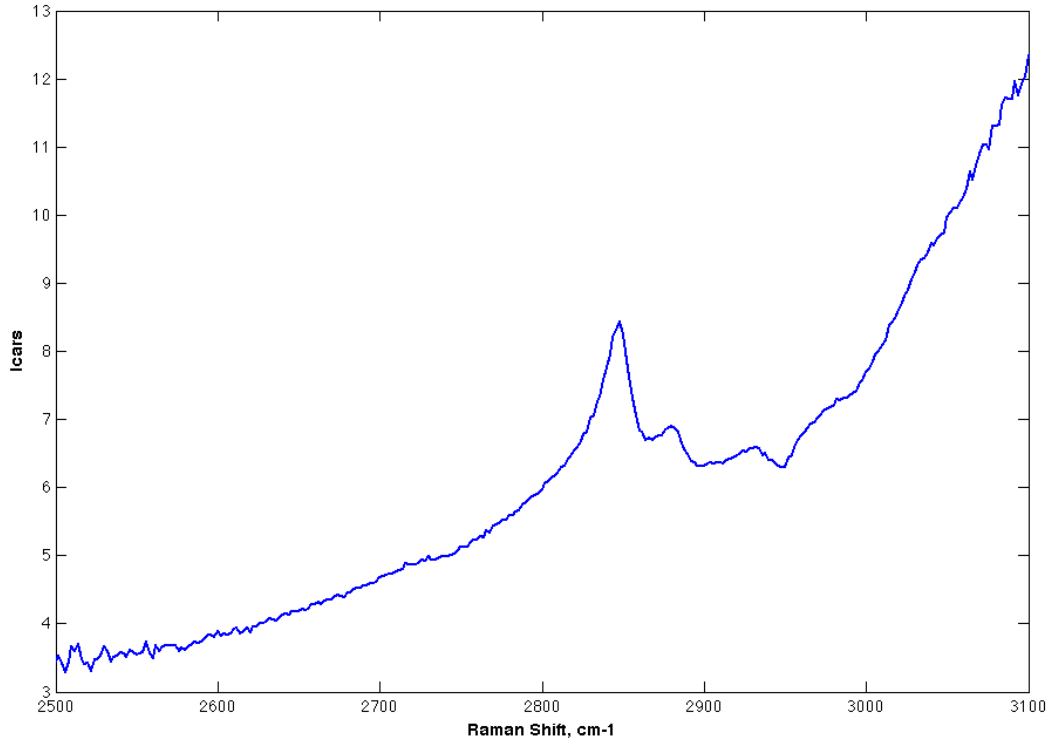

Figure 11. CARS spectrum of the DMPC lipid

Spectral measurements were made on the parts of the spectrum for which the vibrational resonances for the given samples are observed. For DMPC the greatest maxima is observed on 2847 cm^{-1}. For AMP/ADP/ATP mixture the greatest resonance is observed about 1350 cm^{-1}, resonances of separate components of the mixture are visible on 1123 cm^{-1} for ATP and 1100 cm^{-1} for ADP (Figure 10).

Also three unknown spectra were provided. Their line shapes are much more complicated. They are presented in Figures 12,13 and 14.

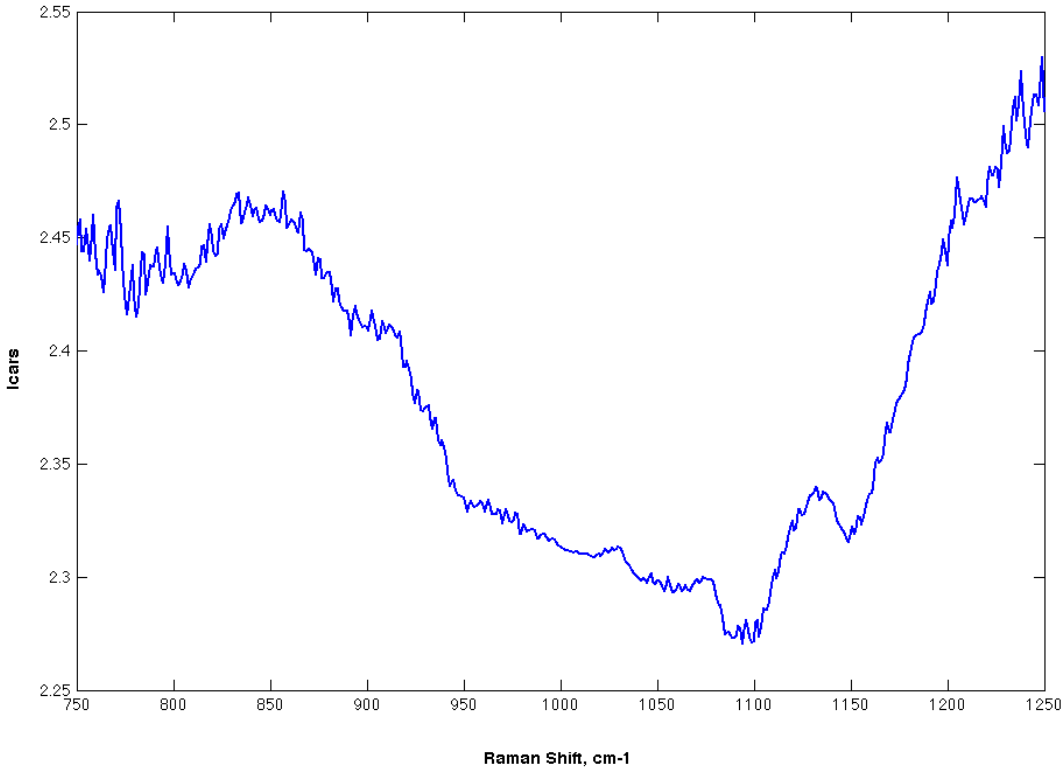

Figure 12. CARS spectrum of the first unknown sample (CCG5C.D)

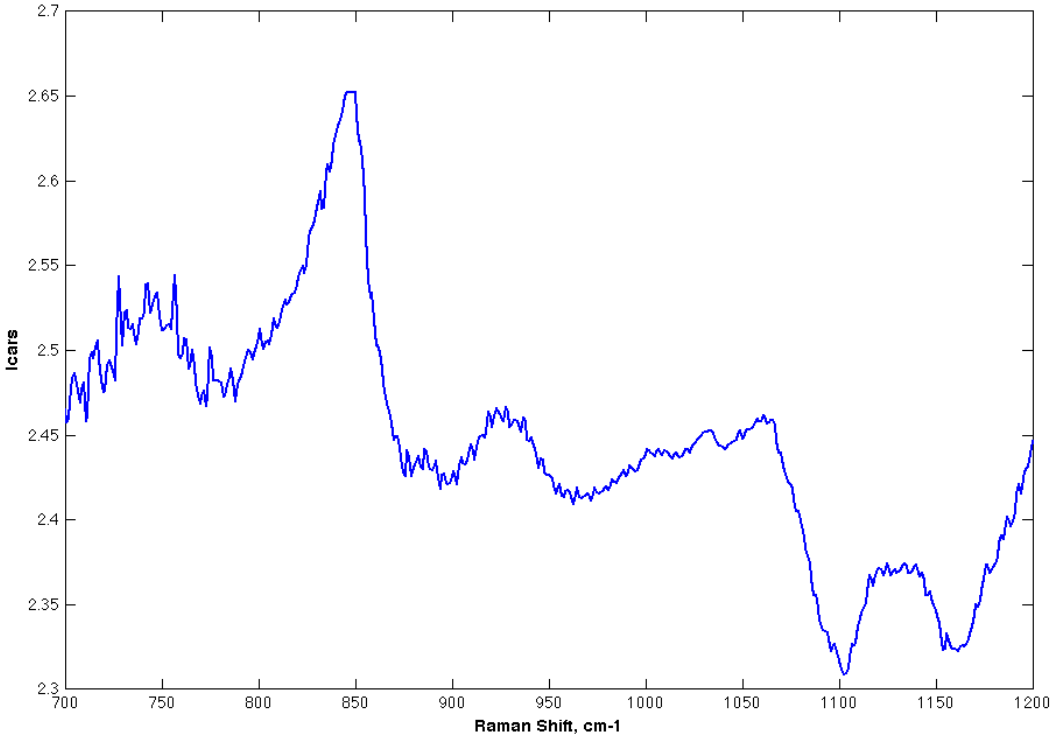

Figure 13. CARS spectrum of the second unknown sample (CCS5CN.D)

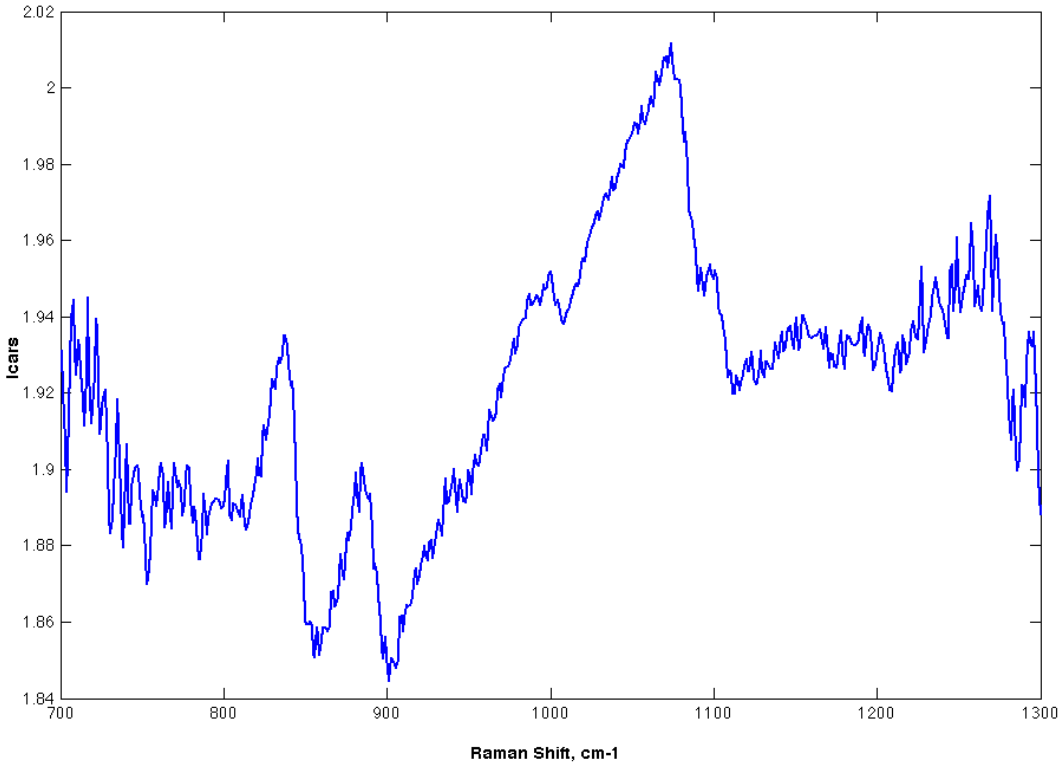

Figure 14. CARS spectrum of the third unknown sample (CCF5CN.D)

6 DEVELOPMENT OF A PHASE RETRIEVAL ALGORITHM

6.1 Statement of the problem

Let's compare the spectra received for the same substances by the spontaneous Raman spectrometer and the CARS spectrometer, i.e. we shall compare Figure 9 with Figure 10. For the spectrum received by Raman spectrometer, the basic resonances, which allows us to determine sample structure are well investigated. CARS spectra generally do not contain any visible resonances in the initial form.

The maximum entropy method has been described above. It allows us to retrieve phase of CARS signal without background correction, using exclusively the intensity measured by a spectrometer. At the moment, this method is well studied and described in several scientific works, including works on its practical application for study of various complicated substances. The program was developed, which applies MEM to a measured CARS spectrum and retrieves phase [25].

Removal of a spectroscopic background is more difficult task. Earlier methods used approximation, being based on the fact, that vibrational resonances are narrow components on a large background.

In the work [18] the method of the wavelet analysis of spectra with the purpose of removal of a low-frequency background and high-frequency noise from spectra was suggested. It was called the “wavelet prism” and was described above.

The main purpose of this work is to apply the maximum entropy method and wavelet analysis for the development of an universal phase retrieval algorithm for CARS spectroscopy.

The input data for the algorithm is a CARS spectrum of intensity, measured by a CARS spectrometer. And the output data is the corresponding calculated spontaneous Raman spectrum, based only on information from CARS measurements.

6.2 Components of the algorithm

1. Calculation of the phase function $\psi(\nu)$ from the intensity spectrum $I_{CARS}(\omega_{as})$, measured by CARS spectrometer using the maximum entropy method. We will receive a phase function which represents the sum of an informative signal and a spectroscopic background as the output data.

2. Selection of an acceptable wavelet. Daubechies wavelets with different scale parameters are usually the best. The task is to select a scale of the function.

3. Use of the multilevel one dimensional discrete fast wavelet transform of the previously calculated phase function $\psi(\nu)$. Decomposition of this function is calculated up to some level *l* (which is usually equal to 6 - 8). The result is presented as number of approximation and detail coefficients (45).

4. According to the "wavelet prism" principle there is an analytical signal at middle frequencies ($f(s)$) and noise at high frequencies. "Prism" decomposes a signal on frequency levels. Then these levels are summed, having excluded the lowermost (the low-frequency filter) and possibly the highest (high-frequency noise filter). We make reconstruction of an initial signal, using only the detailing coefficients received during decomposition and having accepted approximation coefficient equal to zero.

$$f_s = g_1 + g_2 + ... + g_l = G^T d^1 + H^T G^T d^2 + ... + (H^T)^l G^T d^l \quad (50)$$

5. Analysis of the calculated results. If the chosen level of decomposition *l* is too big, the significant contribution to the calculated signal is brought by low frequencies, i.e. there is a spectroscopic background. At magnification of *l*, the signal aspires to take the form of an initial signal. On the other hand, exclusively high frequencies predominate in a signal at small *l*. In that case the calculated signal is considerably distorted and is not suitable for the analysis as a spectrum.

6. On the basis of the analysis, we make a decision, whether the signal is satisfactory for the quantitative analysis of components containing in a sample. If it is not satisfactory, we decrease or increase the decomposition

level l and repeat step 3. If all decomposition levels were tested and are not acceptable, chose different scale parameter of the wavelet and repeat step 2.

6.3 Realization and test of the algorithm

The algorithm was tested on 5 different samples. CARS spectra for these samples were shown above in the experimental section. For one of the samples, the spectrum of spontaneous Raman scattering was provided for comparison.

We will use spectra AMP/ADP/ATP and DMPC for the first experimental part. For the first sample not only the measured spectra of coherent anti-Stokes scattering are accessible but also spectra of spontaneous Raman scattering. For the second sample, some information of a correct Raman line shape is also provided. So, there is a possibility to check of the algorithm on experimental data. Let's make calculations for the spectrum of mixture AMP/ADP/ATP (Figure 9).

Calculations of the phase function by the maximum entropy method (14) was made using the program on the web-site of the developers of this phase retrieval method [25]. Input data was the file containing a spectrum of CARS signal strength (Figure 9), i.e. normalized dependency of CARS signal strength on the Raman shift ($I_{CARS}(\omega_{as})$). As it has been told above the maximum entropy method demands the indication of two parameters: the number of autocorrelation coefficients M and the squeezing parameter *K*.

The squeezing parameter is usually taken 0 or 1. We shall use $K=1$. The initial file has 504 points. Then, according to (20),

$$N=(2\mathrm{K}+1)(N_0-1)+1=(2\cdot 1+1)(504-1)+1=1510$$

Fourier transforms in the maximum entropy method will be made at a discrete number of normalized frequencies $\nu_n=\frac{n}{N}=\frac{n}{1510}$. The number of autocorrelation coefficients is determined as $M\le N/2$. We will take $M=M_{max}$, because noise can be filtered later by wavelet methods and now we are trying to achieve a

maximum approximation of a signal to the original. Thus $M = M_{max} = \frac{1510}{2} = 755$.

Having received the input data, it is possible to make calculations. We upload the file with the spectrum and required parameters to the web-site with the program [13]. The program makes the approximation of the signal using MEM (14-20), and determines the phase function from the calculated approximated spectrum. We will receive a text file, which contains discrete values of the phase function depending on the Raman shift ($\psi(\nu)$). Also the program draws the corresponding graph. Calculated phase function for the spectrum AMP/ADP/ATP is presented in Figure 15.

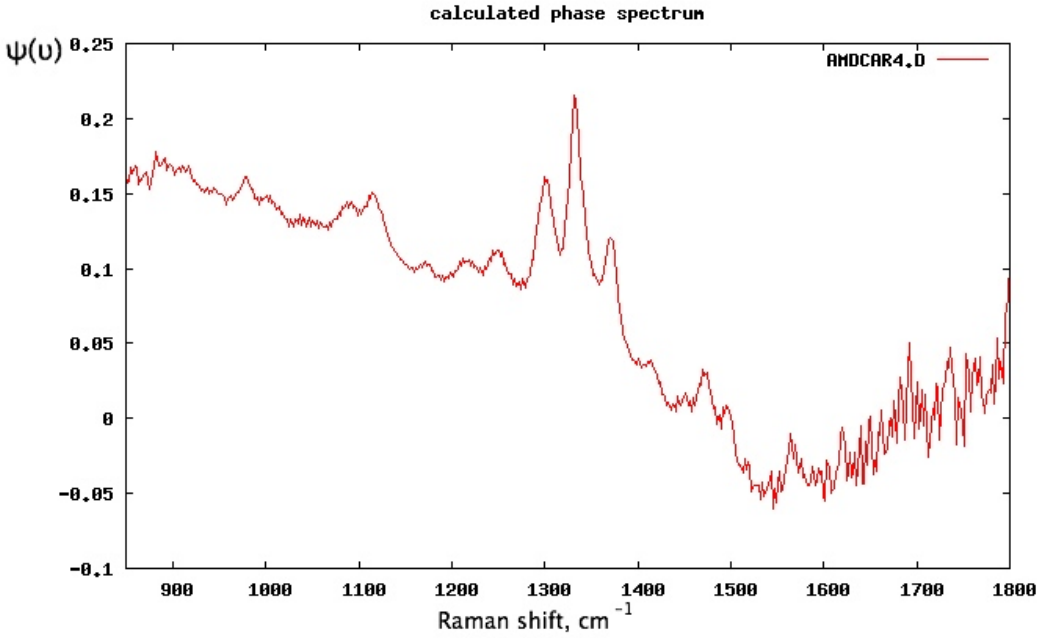

Figure 15. Phase function without background correction of the spectrum of AMP/ADP/ATP

From comparison of the phase function of CARS spectrum (Figure 15) and the spectrum of spontaneous Raman scattering (Figure 10) it is obvious, that the phase function of coherent anti-Stokes scattering has a nonlinear spectroscopic background.

All computations on spectroscopic background removal were made in the mathematical software MATLAB [17]. The phase function of CARS spectrum AMP/ADP/ATP are uploaded into the software (written on the MATLAB internal

language), which was calculated earlier (Figure 15). We also upload the spectrum of spontaneous Raman scattering of the same sample for comparison (Figure 10).

For realization of the wavelet-processing of the signal first of all it is necessary to choose an orthogonal wavelet basis of decomposition. The basic characteristics of the orthogonal wavelet function are smoothness of function, its symmetry, compactness of the carrier in space and frequency areas. The main criteria for a wavelet for our task are maximum smoothness and compactness of a function, because the function should authentically transmit all small details and singularities of an investigated spectrum [26]. After check of set of wavelets with various scales of functions it has been decided, that Daubechies wavelet with the scale of function 15 has the best characteristics for the task. It is presented in Figure 16.

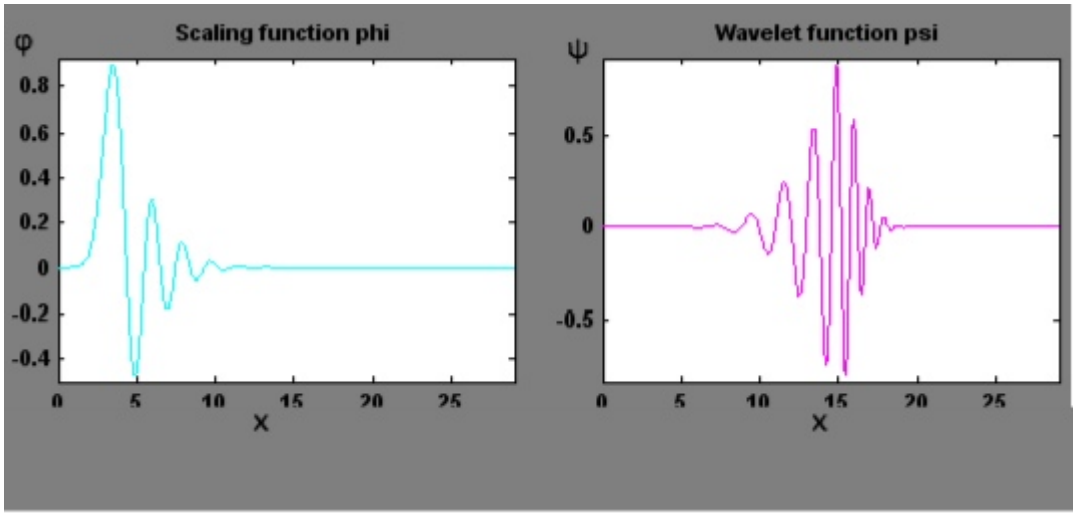

Figure 16. Daubechies wavelet with the scale of function 15

Further for wavelet decomposition of a signal it is necessary to choose a level of decomposition, i.e. how many times wavelet transforms will be made. The number of decomposition coefficients depends on it. We shall accept a level equal $l = 8$.

Let's note, that the better result with less signal distortion is observed, when we fuse the original signal with its mirror image.

The function of multilevel wavelet transform from MATLAB

$[C,L]=wavedec(y,l,wwl)$ was used, where y is the initial function (phase function), l is the necessary level of decomposition (equal 8), *wwl* is the wavelet-basis of decomposition ("db15"). Calculated vectors C and L contain a set of approximation and detail coefficients which will be used for inverse decomposition of a signal.

This set of wavelet coefficients allows us to utilize the method of the "wavelet prism", which consists of decomposition of the signal on wavelet frequencies for its analysis on presence of a background or noise. The high-frequency component is separated from the signal at each next wavelet transform. At magnification of the level of decomposition, frequencies of these component fall. After separating last high-frequency component at the final (l^{th}) level of decomposition, l^{th} branch of the approximation coefficients also remains which represents ultra-low frequencies.

We restore a signal, using only detail coefficients (on one branch of coefficients on a signal), and also the l^{th} branch of approximation coefficients. For this purpose the function $x_n=wrcoef(type,C,L,wwl,n)$, where $type='a'$ for reconstruction on a branch of approximation coefficients and $type='d'$ for reconstruction on a branch of detail coefficients, n is the level of decomposition (from 1 up to 8 for detail coefficients and 8 for approximation coefficients) is used. Thus we obtain nine functions, representing "prismatic" decomposition on wavelet frequencies.

Nine signals are presented in Figure 17. It is easy to notice, that the first graph reflects the contribution of the highest frequencies, and last reflects the lowest. The spectroscopic background of a signal places on the lowest frequencies. Here the background is at the last graph in the figure. Now it is enough to restore the initial signal, using only eight branches of detail coefficients, in other words, to sum and then to normalize functions at n equal from 1 up to 8 Thus, the signal which does not have an ultra-low wavelet frequency will be received. This signal should not contain the spectroscopic background. The result of the low frequency removal from the phase function is presented in Figure 18.

Here we observe some distortion at the shift between 900 and 1000. These possibly could be avoided, if the spectrum with higher bandwidth is provided.

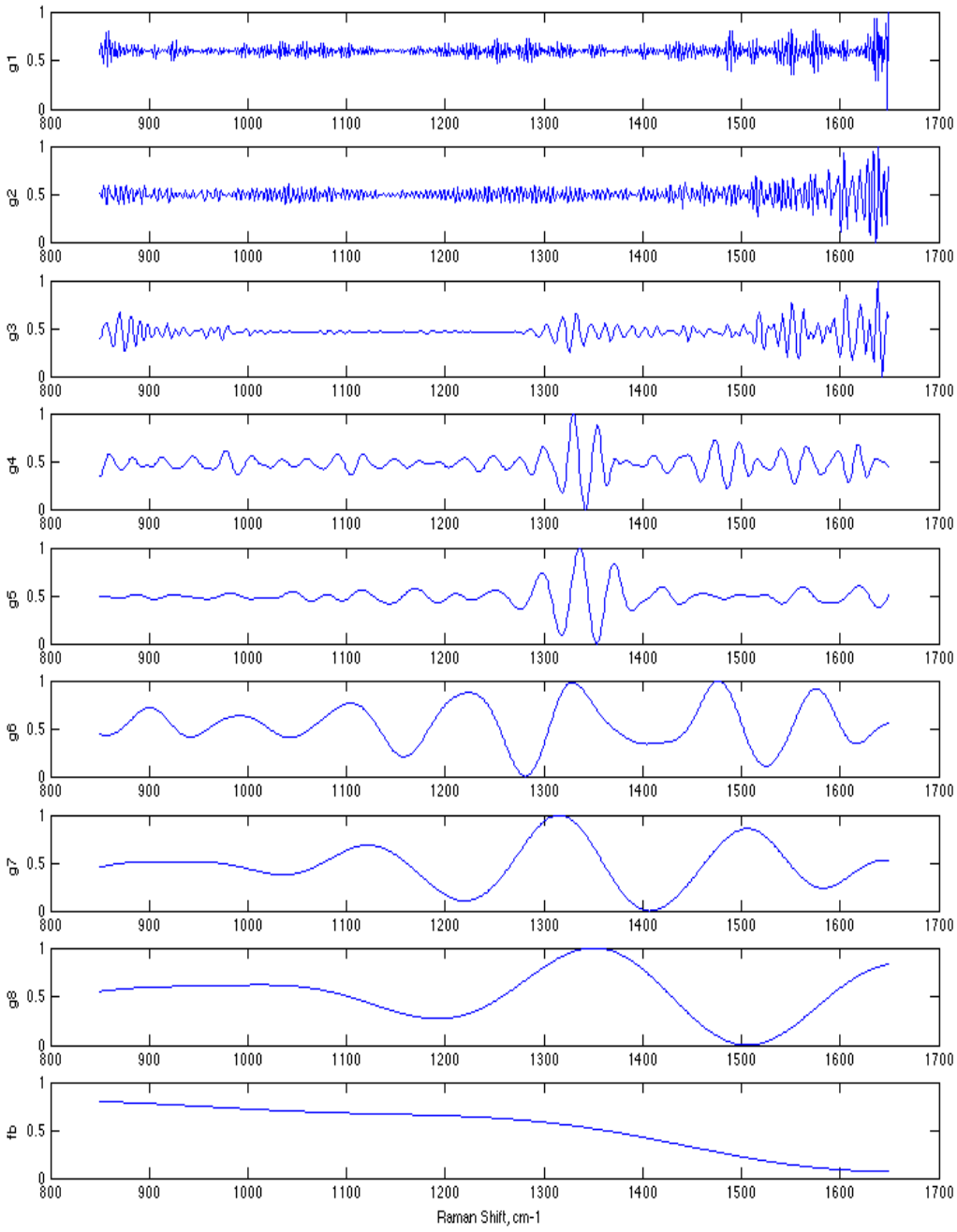

Figure 17. Realization of the method of a "wavelet prism" for the spectrum of AMP/ADP/ATP

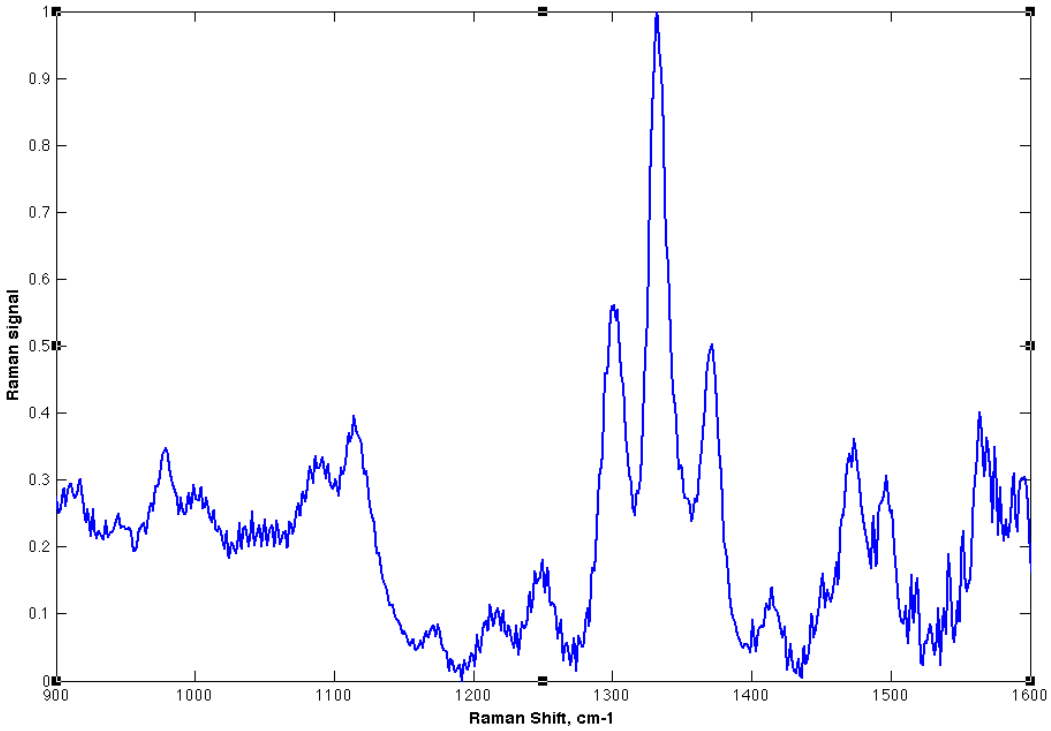

Figure 18. Estimated Raman spectrum of mixture AMP/ADP/ATP after spectroscopic background removal

Let's estimate an optimality of choice of the decomposition level. The resulting spectra after application of the described method at three various levels of wavelet decomposition: 9, 8 and 7 are shown in Figure 19. Calculated CARS signal is presented in comparison with the spectrum of spontaneous Raman scattering (from Figure 10).

At the decomposition level l = 9 the contribution of the low-frequency background component of a signal is still significant. The spectrum is inclined. On the other hand, if to accept the decomposition level l = 7, important mid-frequency components are deleted from the spectrum. We observe distortion of the signal by dominance of high frequencies. Thus, the decomposition level equal eight approximates the form of the signal of CARS spectrum to the form of the signal of spontaneous Raman spectrum the best way.

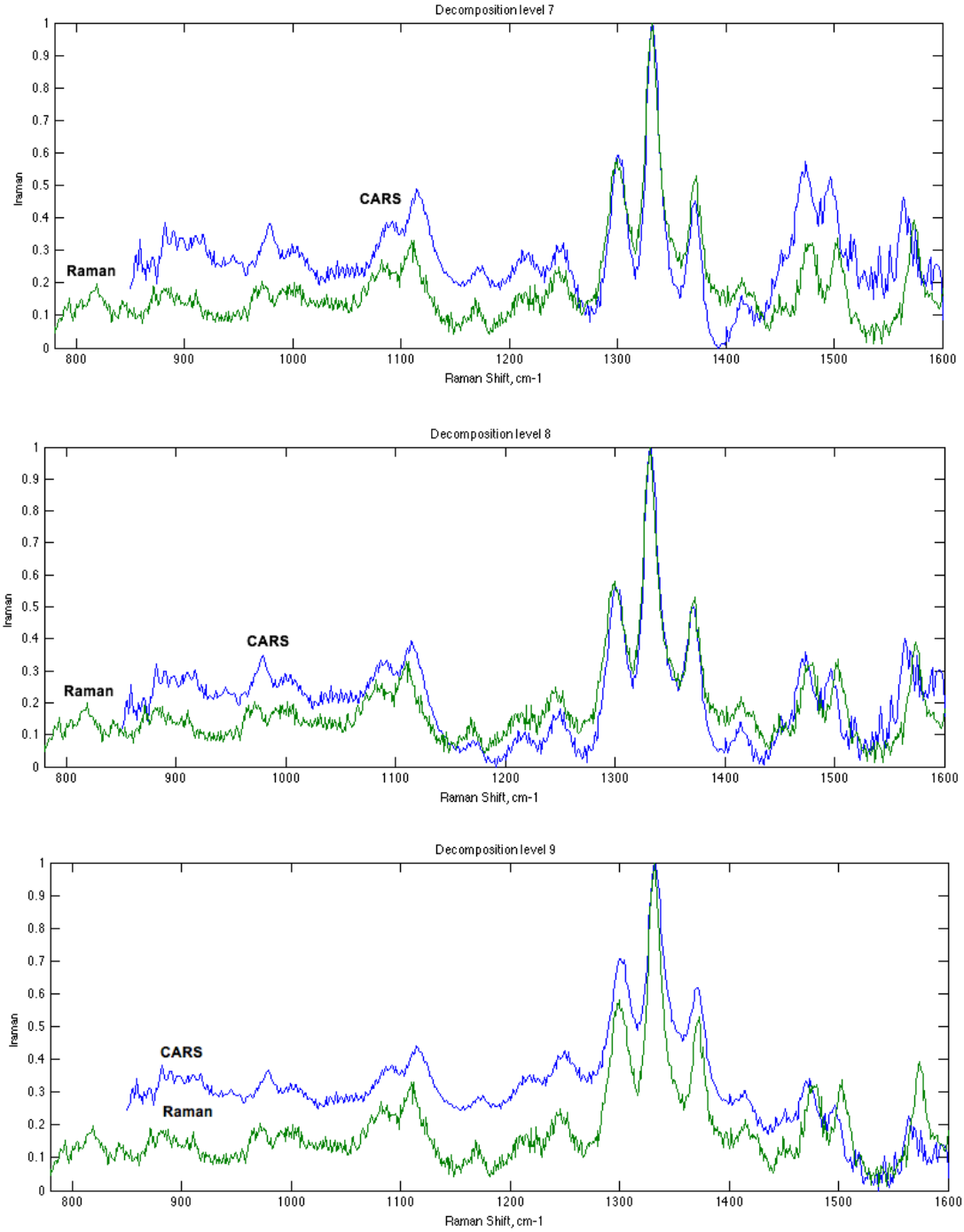

Figure 19. Estimated Raman spectrum of mixture AMP/ADP/ATP (marked as “CARS”) at three various decomposition levels in comparison with the spectrum spontaneous Raman scattering (marked as “Raman”)

We shall note, that the chosen decomposition level is generally fair only for the given spectrum line shape (AMP/ADP/ATP) and for the given spectral resolution (1 cm^{-1} per measurement). I.e. the optimum decomposition level depends on the form of a spectrum line shape of an investigated signal, and also from a spectral resolution of

the lead measurement.

Automatic definition of the necessary decomposition level is possible if the signal of spontaneous Raman scattering, on which it is possible to be guided, is known or if more than one spectrum are provided for the same sample (it is possible to use Shannon entropy in such case). However, initially the method was developed for cases when such comparison to lead it is impossible, since CARS equipment allows to receive a “picture” of a condition of substance in a very short time interval, for example, during a fast multistage chemical response.

Thus, the level of expansion is chosen manually. It does not take much time, because the number of possible variants is usually less than ten. It is possible to calculate instantly all and of them to choose the most suitable for the subsequent research of a spectrum.

Let's consider the test of the DMPC substance. An optimum decomposition level is 7 for CARS signal of DMPC. The result was calculated like shown above. MEM and “wavelet prism” were used.

For the method of maximum entropy the following parameters were used:

$N_0 = 301$

$M = M_{max} = 450$

$K = 1$

The result data from the MEM program for evaluation of phase function is presented in Figure 20. Then we make wavelet decomposition through the “prism” (Figure 21). Like in the previous example, we will remove the last low-frequency component from the signal and make the reverse wavelet transform. Thus, we will receive the spectrum without spectroscopic background. The CARS spectrum of this substance after spectroscopic background removal is shown in Figure 22.

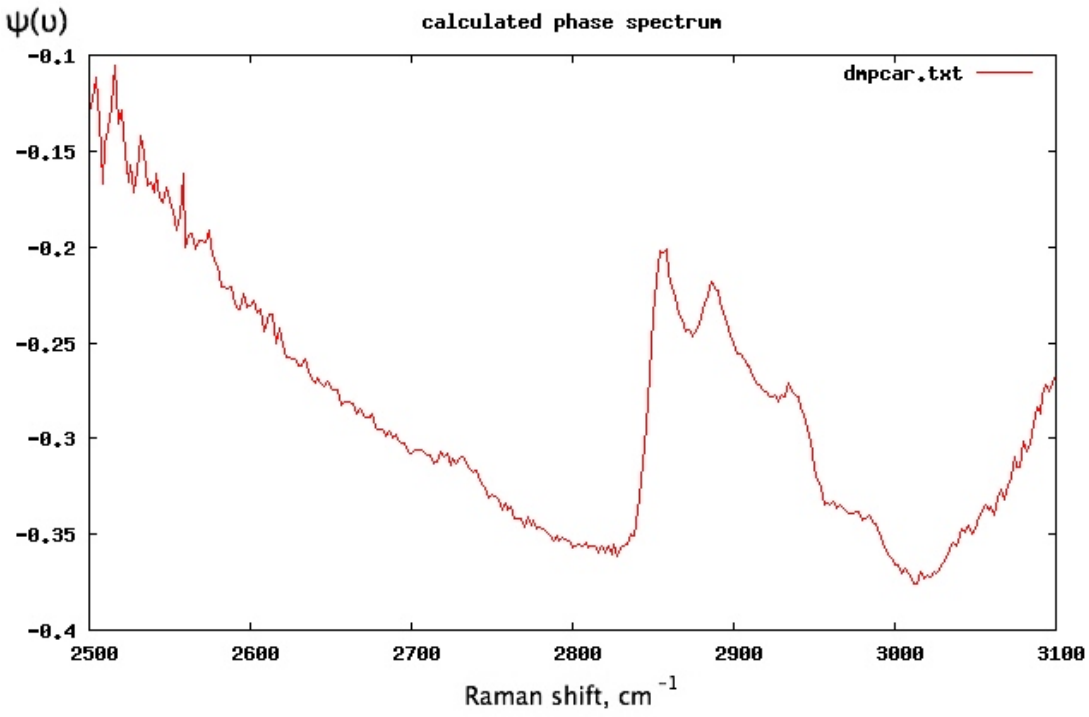

Figure 20. Phase function with a spectroscopic background of the DMPC spectrum

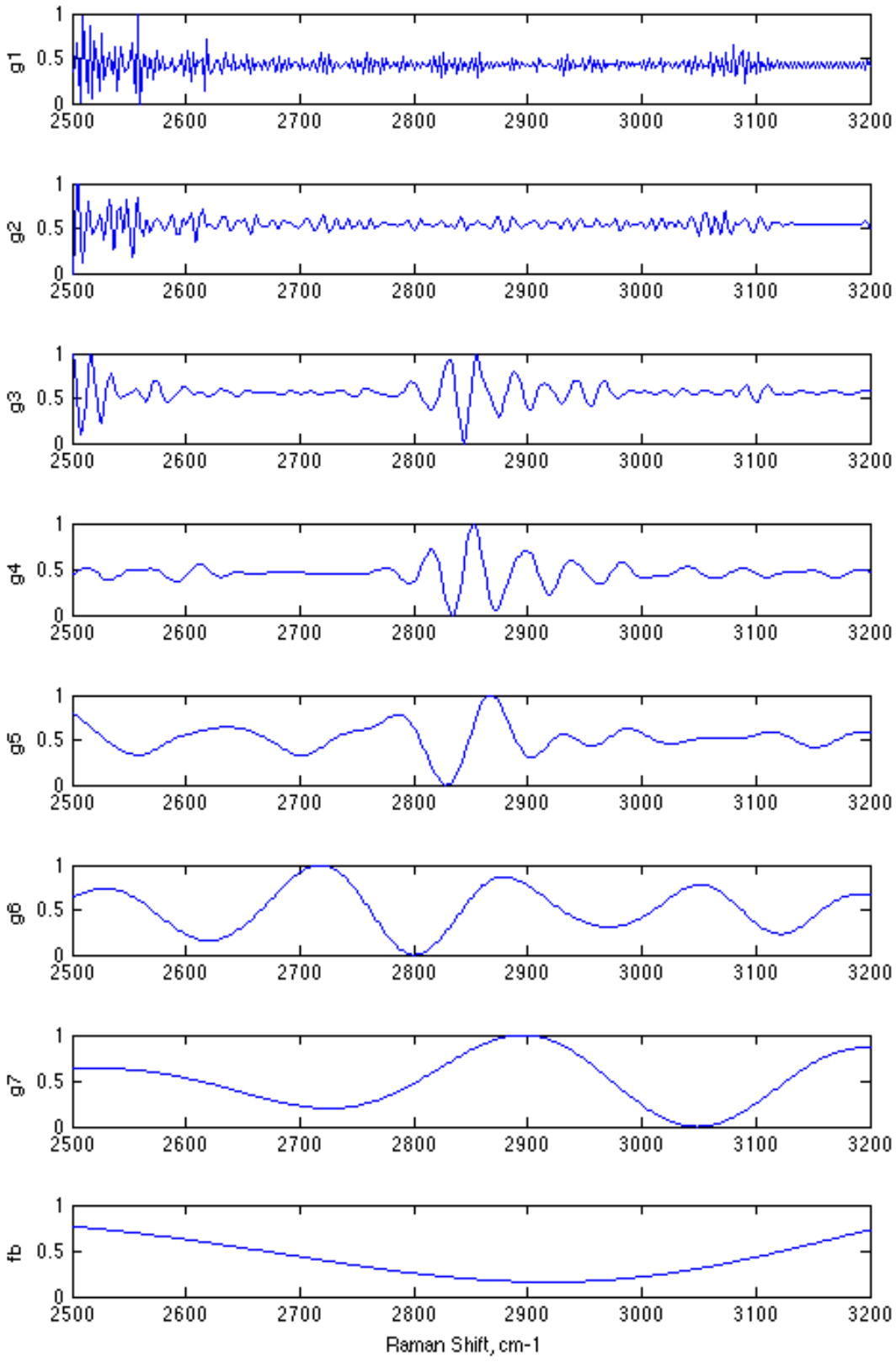

Figure 21. Realization of the method of a "wavelet prism" for the spectrum of DMPC

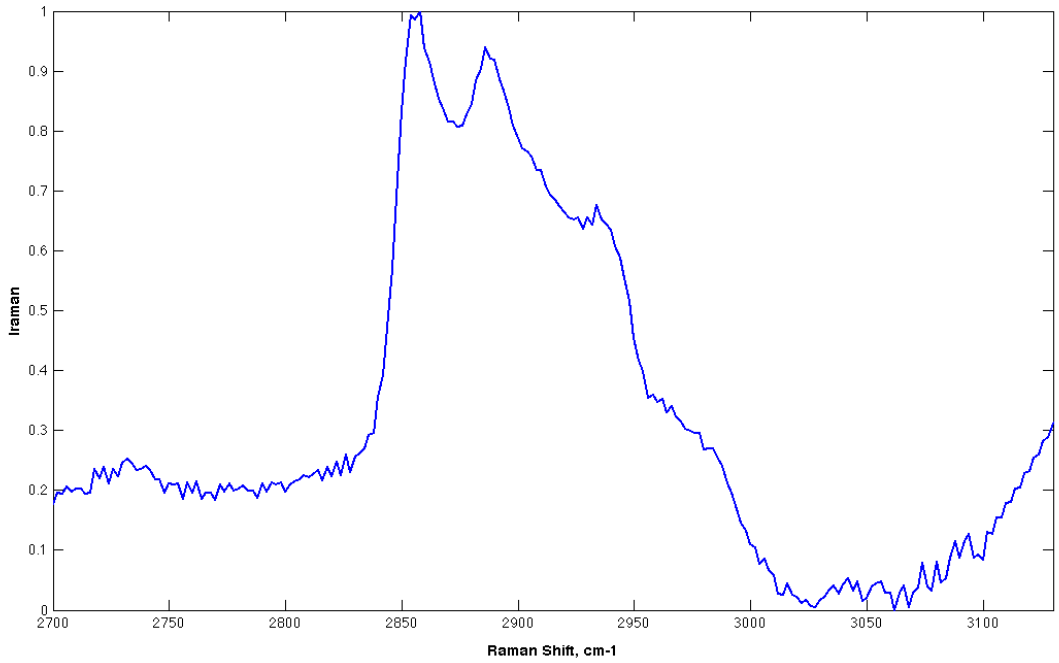

Figure 22.Estimated Raman spectrum for DMPC lipid

6.4 Wavelet decomposition of more complicated spectra

The spectra in Figures 12,13 and 14 are more difficult to analyze, because absolutely no additional information is provided about vibrational resonances of these substances. We will try to apply the algorithm to remove spectroscopic background from these spectra.

Let's skip the MEM part and consider only wavelet transforms of the signals to remove spectroscopic backgrounds of their MEM phases. In Figures 23, 24 and 25 MEM phases of these samples for background removal are provided. On the basis of these MEM phases we can suggest that these samples have some kind of sine wave background.

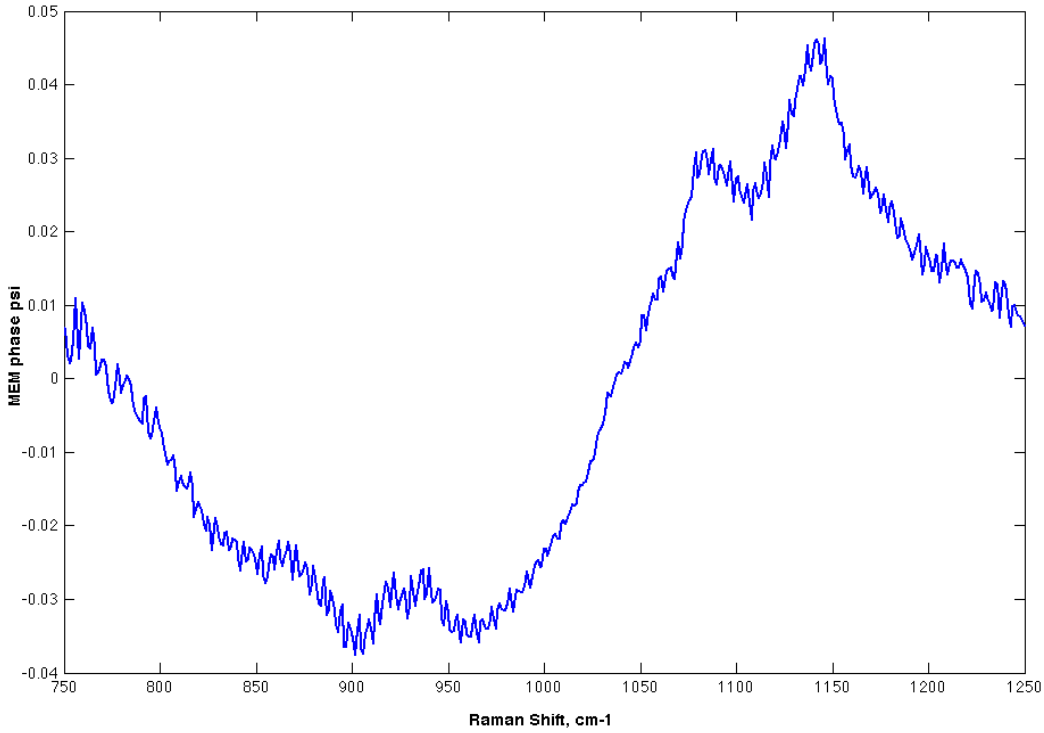

Figure 23. Phase function of the first unknown sample (CCG5C.D)

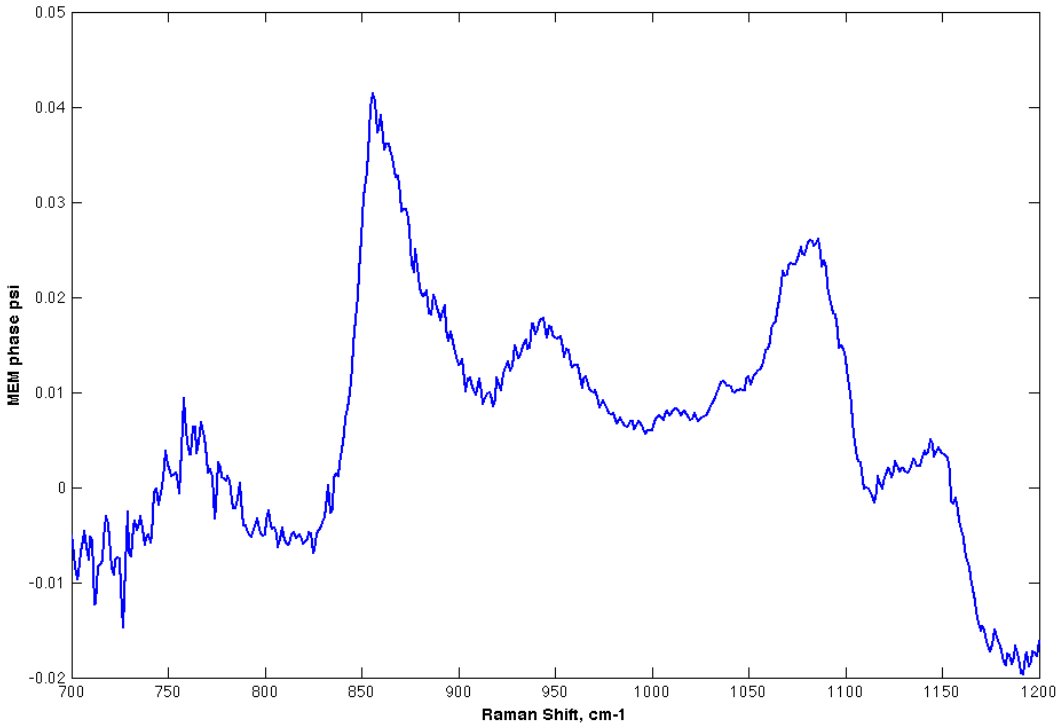

Figure 24. Phase function of the second unknown sample (CCS5CN.D)

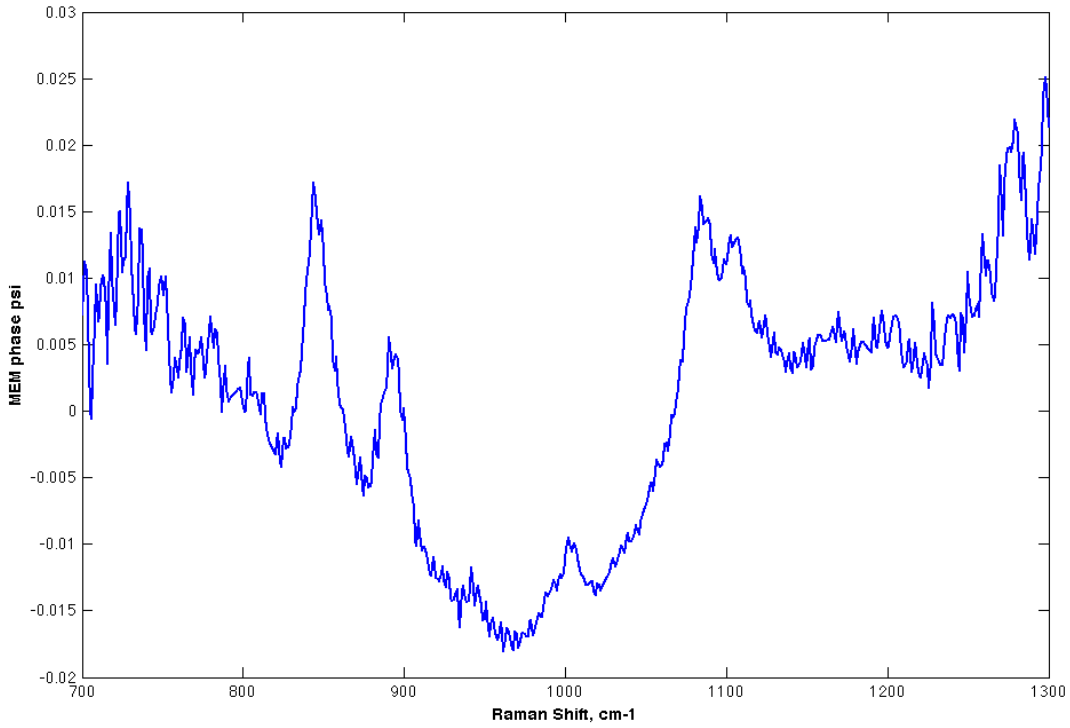

Figure 25. Phase function of the third unknown sample (CCF5CN.D)

Let's process the first sample. We will use the “wavelet prism” method to decompose the signal on frequencies up to level 7 (Figure 26). If we compare the gained decomposition to the previous samples (Figures 17 and 21), it is visible, that the spectrum has the significant noise component. This noise part is arranged in high-frequency components g1 and g2. Thus, it is possible to remove noise without significant distortion of the spectrum. For this purpose we shall remove the detail components g1 and g2 at the inverse transform of the signal. Calculated Raman spectrum with elimination and without elimination of noise is presented in Figure 27.

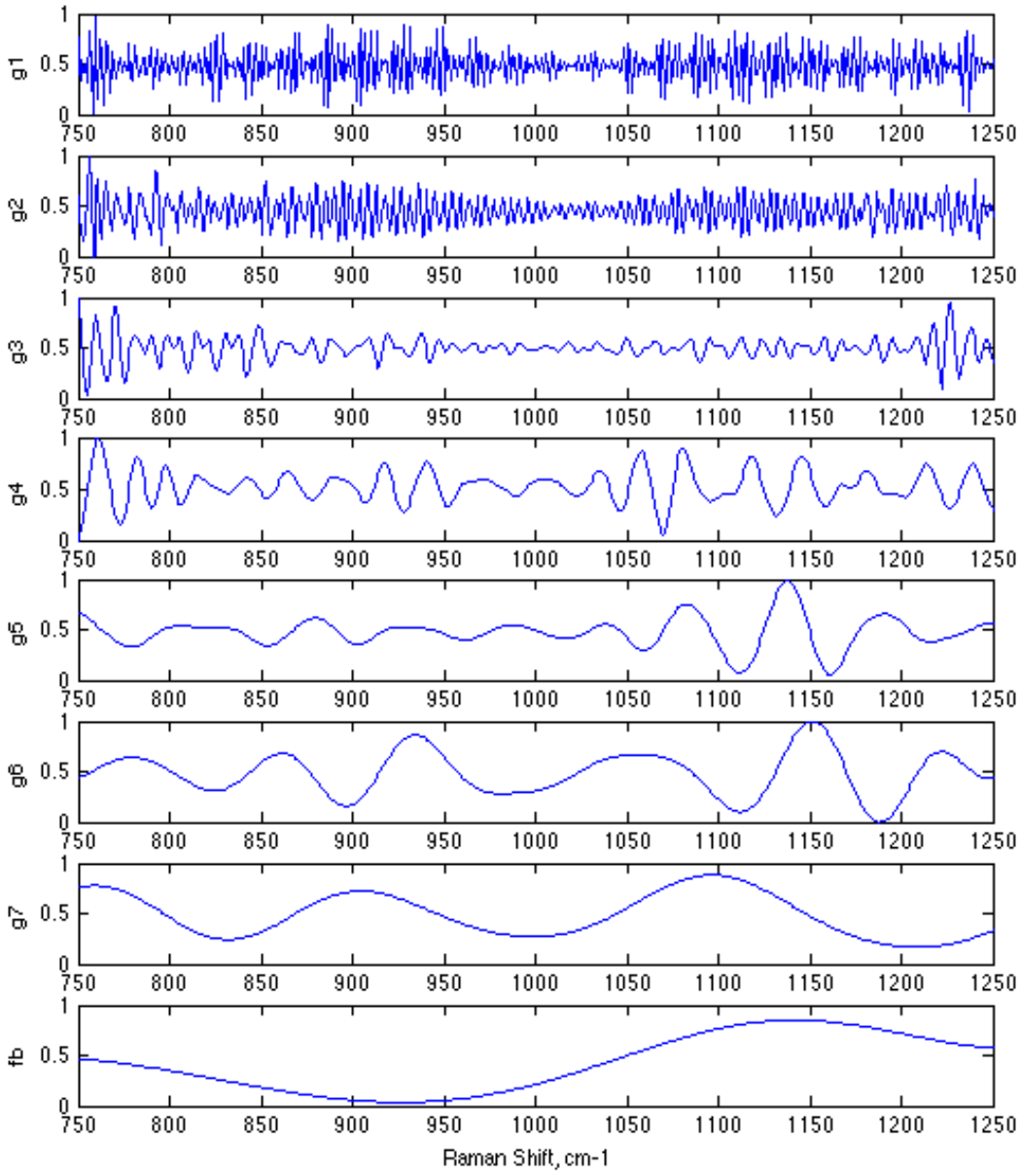

Figure 26. The method of a “wavelet prism” for the first sample (CCG5C.D)

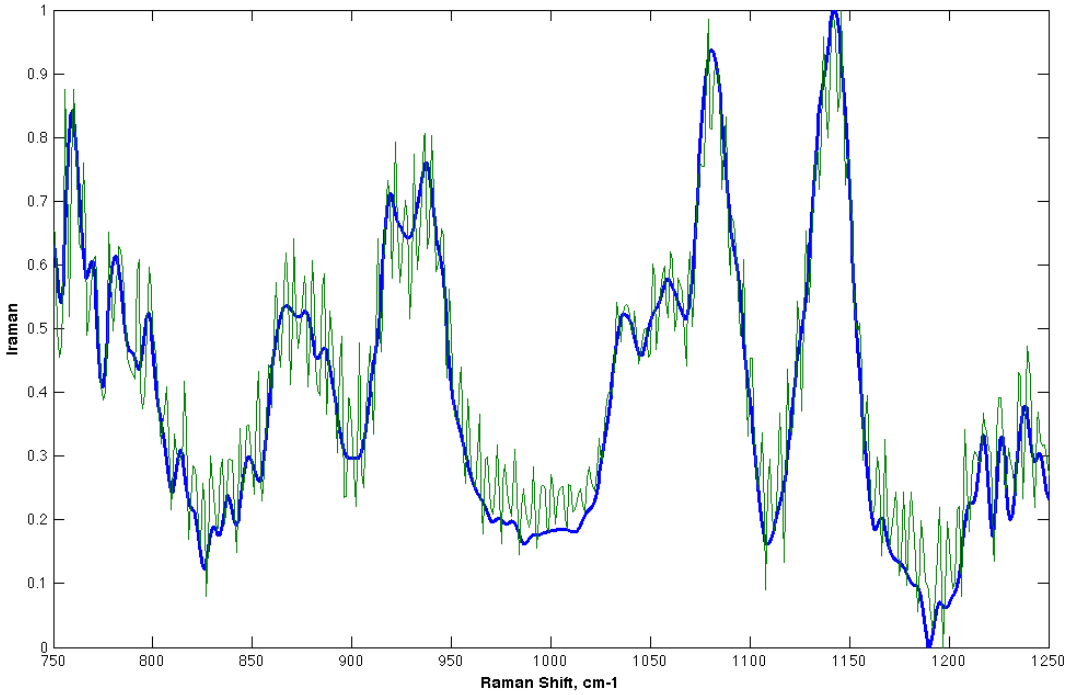

Figure 27. Estimated Raman spectrum for the first sample (CCG5C.D) with and without noise removal

The second sample does not contain much noise, but has a different problem. It is impossible to get an acceptable background removal with the wavelet used previously (“db15”). So, the scale parameter of the Daubechies wavelet has been taken equal 8 (“db8”). The decomposition level has been also taken $l = 8$.

The “wavelet prism” decomposition of the second sample using selected wavelet “db8” is shown in Figure 28. The result of background removal for the second spectrum is shown in Figure 29 in two cases: with use of the wavelet "db15" and the wavelet “db8” .

The best result here is observed without addition of the mirror image to the spectrum. Another problem arises that we can not check where all minima are detected correctly. For example, there is a possibility that the minimum near 915 cm^{-1} should be near zero on the I_{Raman} axis.

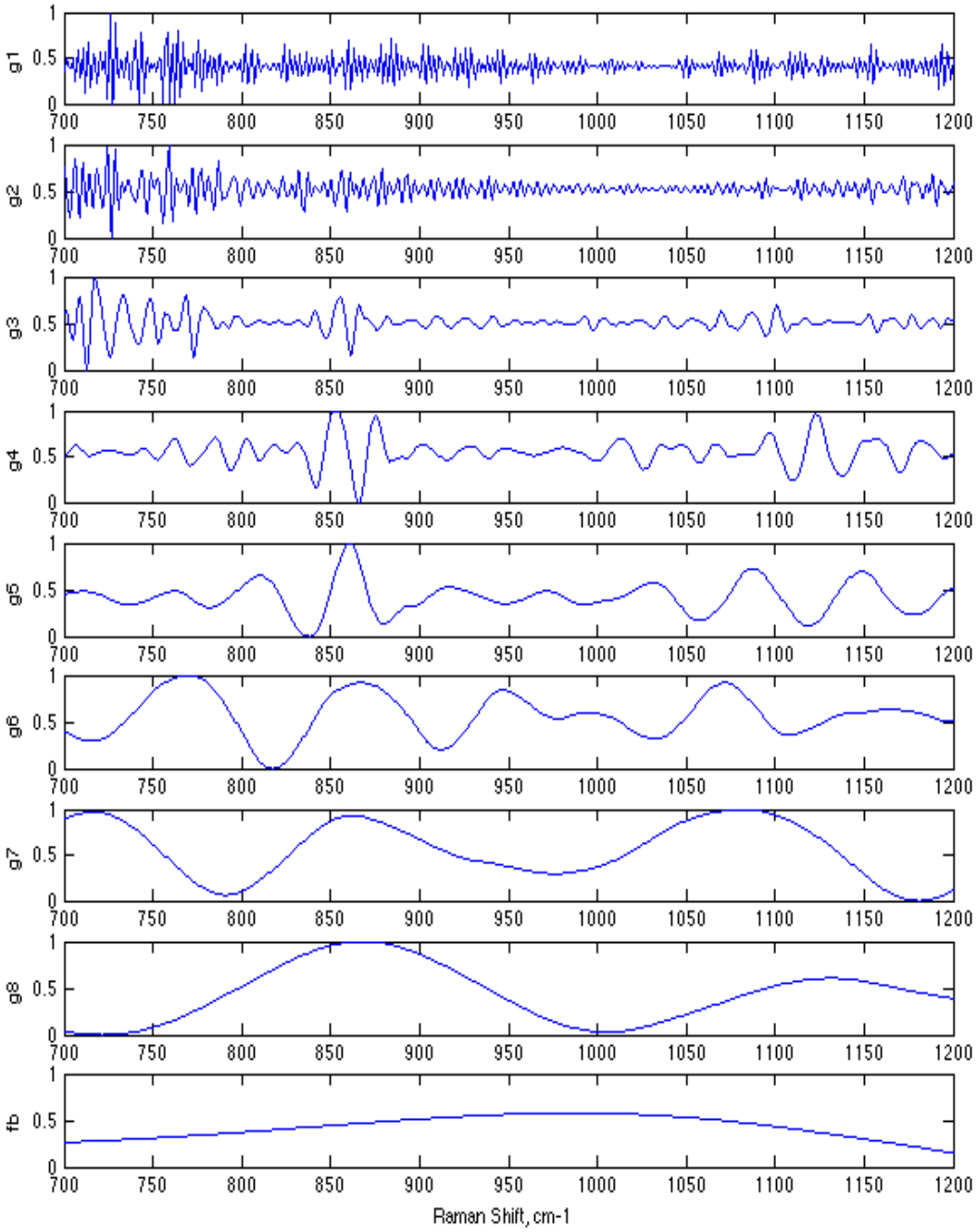

Figure 28. The method of a “wavelet prism” for the second sample (CCS5CN.D) using Daubechies wavelet with the scale parameter 8 (“db8”)

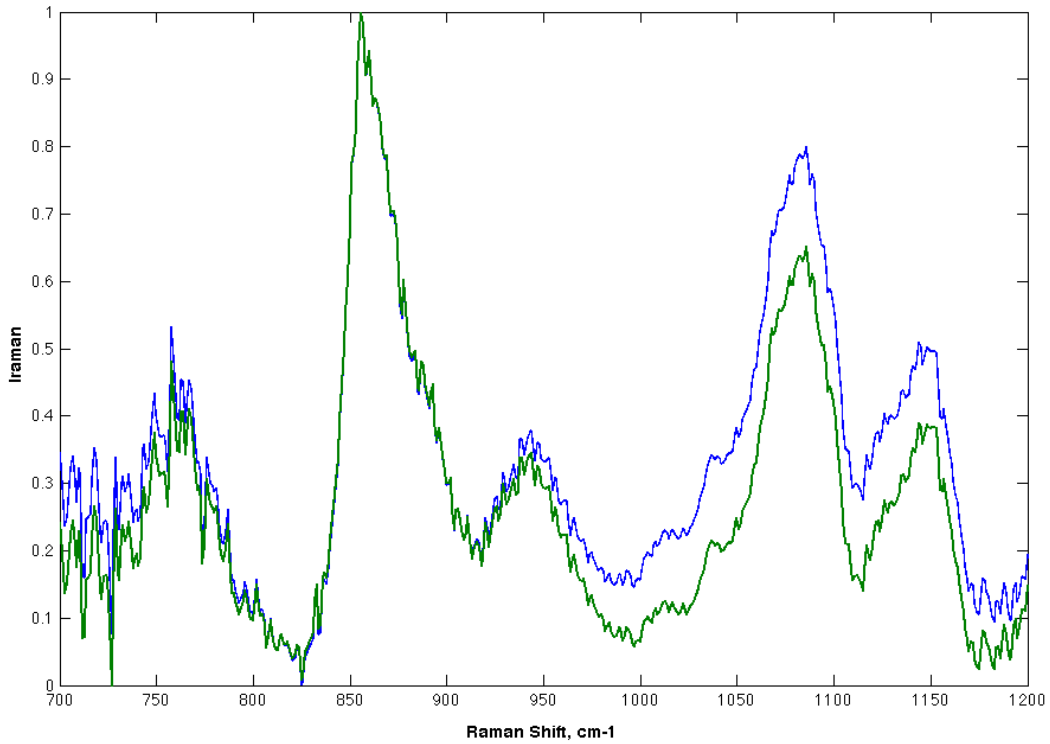

Figure 29. Estimated Raman spectrum for the second sample (CCS5CN.D) using wavelets with different scales: Daubechies 15 (upper line) and Daubechies 8 (lower line)

For the decomposition of the third sample's spectrum, the Daubechies wavelet with the scale parameter 8 was used again. The decomposition level was chosen as 7. “Prism” decomposition again is shown in Figure 30.

Noise was filtered in this spectrum by removing the first detail component g1. The resulting Raman spectrum is shown in Figure 31.

Thus, the background correction was rather successfully applied to these three samples. Also the possibility of noise removal from the spectra was investigated successfully.

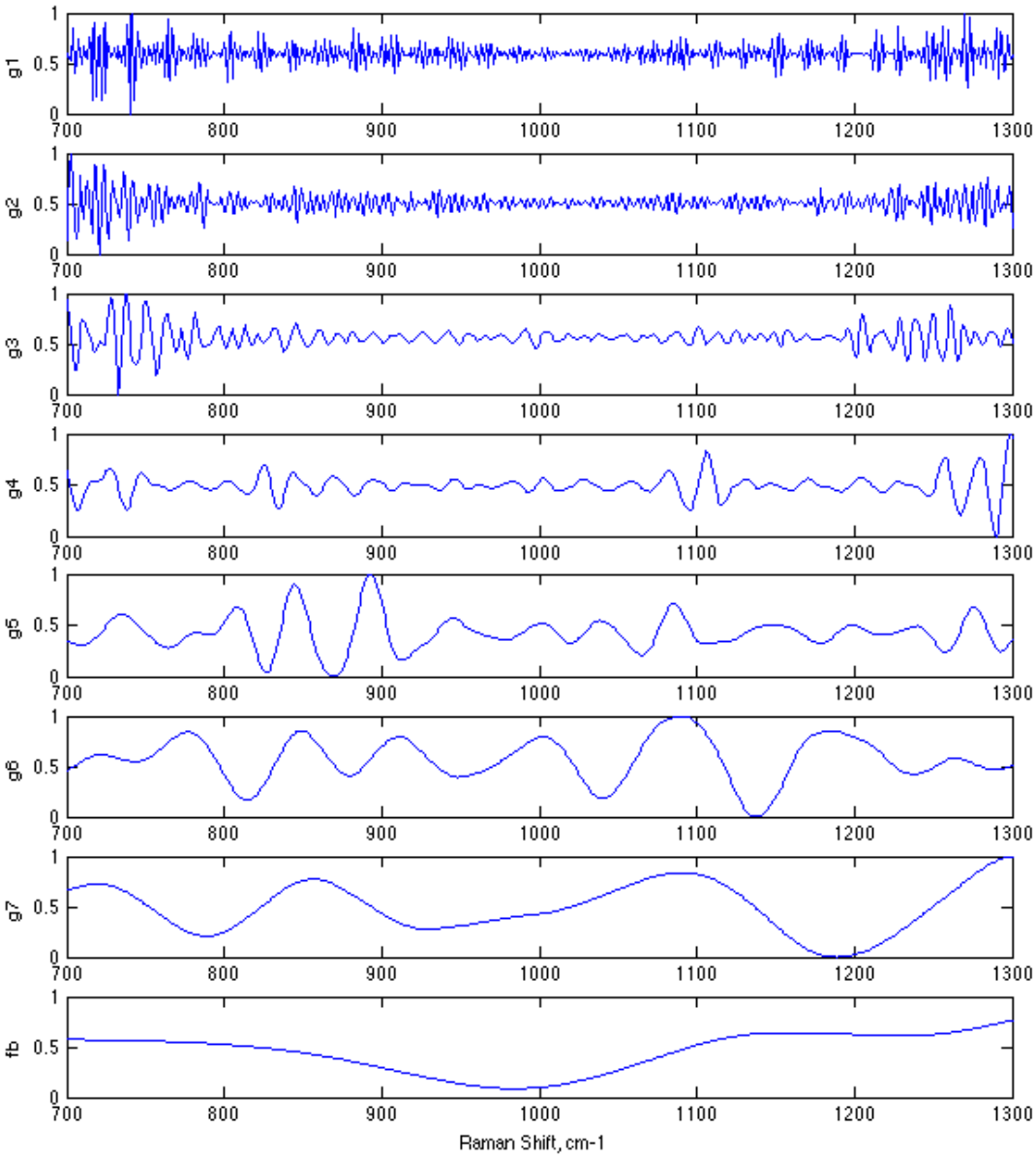

Figure 30. The method of a “wavelet prism” for the third sample (CCF5CN.D) using Daubechies wavelet with the scale parameter 8 (“db8”)

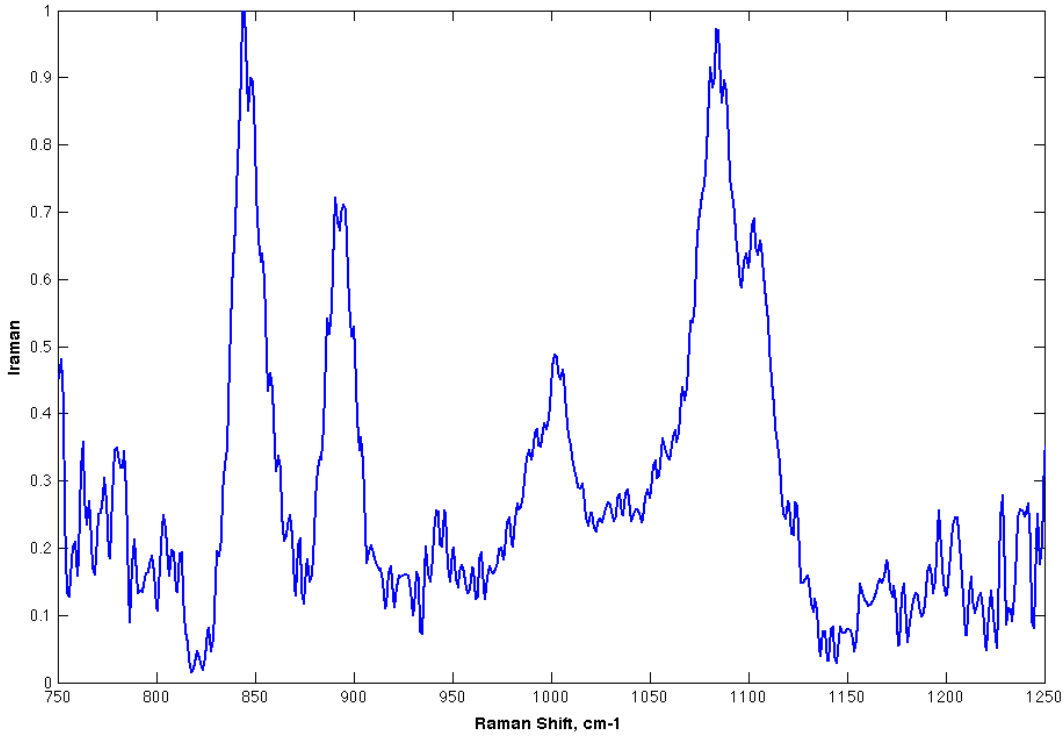

Figure 31. Estimated Raman spectrum for the third sample (CCF5CN.D)

7. CONCLUSIONS

The objective of this work was to develop a new phase retrieval algorithm and technique for CARS spectrometry. That is to retrieve a line shape similar to the spontaneous Raman line shape from a CARS spectrum. The algorithm utilizes the maximum entropy method for phase retrieval and wavelet decomposition for spectroscopic background removal.

It has been shown that suggested approach can be applied to the spectra of different substances. The wavelet part of the algorithm requires selection of the type of a wavelet with its scale parameter (if needed) and the decomposition level. The algorithm is based on the idea, that wavelet decomposition can split a signal into different frequencies. Spectroscopic background, analytical signal and noise are located in different frequencies, so they can be easily separated from each other.

When the algorithm was tested on five different substances, it was noticed, that the wavelet method can not sometimes provide the same accuracy as manual fitting of a background. The result can be improved by selecting a different wavelet, but not in all cases. The main advantage is that the algorithm can have easy realization in a computer program. All calculations were made in MATLAB. It is also possible to write a program which can provide additional corrections to a resulting phase function.

The results of the thesis give important information about specific features of CARS spectra. The developed method can be used in wide range of scientific experiments which use methods of multiplex coherent anti-Stokes scattering spectroscopy. It can find application in biophysics [22,27-29], biology and in examinations of properties of materials [30,31].

REFERENCES

1. "The Raman effect", http://portal.acs.org/portal/acs/corg/content?_nfpb=true&_pageLabel=PP_ARTICLEMAIN&node_id=924&content_id=WPCP_007605&use_sec=true&sec_url_var=region1

2. W. S. Gorelik, "Kombinacionnoe rassejanie sveta" ("Combinational scattering of light", in Russian), Soros Educational Journal, №6, 91-96 (1997)

3. A. I. Fishman, "Spektroskopija kogerentnogo antistoksova rassejanija sveta" ("Spectroscopy of coherent scattering of light", in Russian), Soros Educational Journal, №4, 105-110 (2001)

4. N. B. Delone, "Nelinejnaja optika" ("Nonlinear optics", in Russian), Soros Educational Journal, №3, 94-99 (1997)

5. W. Hubschmid, R. Bombach, "Laser spectroscopy in combustion research", Introduction to numerical methods in combustion research, Ercoftac summerschool, 4.1-4.12 (2002)

6. N. I. Korotneev, "Interferencionnye javlenija v kogerentnoj aktivnoj spektroskopii rassejanija i poglowenija sveta: gologaficheskaja mnogomernaja spektroskopija" ("Interference effects in the coherent active spectroscopy of scattering and absorption of light: the holographic multivariate spectroscopy", in Russian), Advances in Physical Sciences, vol. 152, no.3, 493-518 (1987)

7. G. I. Petrov, R. Arora, V. V. Yakovlev, X. Wang, A. V. Sokolov, M. O. Scully, "Comparison of coherent and spontaneous Raman microspectroscopies for noninvasive detection of single bacterial endospores", PNAS, vol.104, no.19, 7776-7779 (2007)

8. H. A. Rinia, M. Bonn, M. Müller and E. M. Vartiainen, "Quantitative CARS spectroscopy using the maximum entropy method: the main lipid phase transition", Submitted to: JOSA B, (2006).

9. H. A. Rinia, M. Bonn, and M. Muller, “Quantitative multiplex CARS spectroscopy in congested spectral regions”, J. Phys. Chem. B 110, 4472-4479 (2006).

10. E. M. Vartiainen, H. A. Rinia, M. Müller, and M. Bonn, “Direct extraction of Raman line-shapes from congested CARS spectra”, Opt. Express 14, 3622-3630 (2006)

11. A. M. Jeltikov, “Femto- i attosekundnaja spektrohronografija” (“Femto- and attosecond spectrochronography”, in Russian), MSU, Phys. faculty

12. E. M. Vartiainen, K. E. Peiponen, and T. Tsuboi, “Analysis of coherent Raman spectra,” J. Opt. Soc. Am. B 7, 722- (1990)

13. E. M. Vartiainen, “Phase retrieval approach for coherent anti-Stokes Raman scattering spectrum analysis”, J. Opt. Soc. Am. B 9, 1209-1214 (1992).

14. E. M. Vartiainen, K.-E. Peiponen, and T. Asakura, “Phase retrieval in optical spectroscopy: resolving optical constants from power spectra”, Appl. Spectrosc. 50, 1283-1289 (1996)

15. A. V. Davydov, “Vejvlety. Vejvletnyj analiz signalov” (“Wavelets, wavelet-analysis of signals”, in Russian), http://prodav.narod.ru/wavelet/index.html (2007)

16. N. M. Astafieva, “Vejvlet-analiz: osnovy teorii i primery primenenija” (“Wavelet analisys: the basics of theory and examples of application”, in Russian), Advances in Physical Sciences, Vol. 166, №11, 1145-1170 (1996)

17. N.K. Smolentsev, “Osnovy teorii vejvletov. Vejvlety v MATLAB.” (“Basics of the wavelet theory. Wavelets in MATLAB”, in Russian), DMK-Press (2005)

18. H. W. Tan, S. D. Brown, “Wavelet analysis applied to removing non-constant, varying spectroscopic background in multivariate calibration”, Journal of Chemometrics. 16:228–240 (2002)

19. S. G. Mallat, “A theory for multiresolution signal decomposition: the wavelet representation”, IEEE Pattern Anal. Machine Intell, 11:674-693 (1989)

20. J. X. Cheng and X. S. Xie, “Coherent Anti-Stokes Raman Scattering Microscopy: Instrumentation, Theory, and Applications”, J. Phys. Chem. B 108, 827-840 (2004).

21. Cheng, A. Volkmer, L. D. Book, and X. S. Xie, “An epi-detected coherent anti-Stokes Raman scattering (E-CARS) microscope with high spectral resolution and high sensitivity”, J. Phys. Chem. B 105, 1277-1280 (2001).

22. M. Michiel, S. Juleon, “Imaging the thermodynamic state of lipid membranes with multiplex CARS microscopy”, M.. J. Phys. Chem. B. 2002. 106, № 14, 3715–3723.

23. M. D. Duncan, J. Reintjes, and T. J. Manuccia, "Scanning coherent anti-Stokes Raman microscope," Opt. Lett. 7, 350- (1982)

24. Nirit Dudovich, Dan Oron, Yaron Silberberg, “Single-pulse coherently controlled nonlinear Raman spectroscopy and microscopy”, letters to nature, vol. 418, 512-514 (2002)

25. M. Müller, “Maximum Entropy Method for phase retrieval of CARS data”, http://wwwmc.bio.uva.nl/~muller/cars/

26. Y.S. Belehov, V.A. Tkal, A.O. Okunev, M.N. Petrov, “Ustranenie fonovoj neodnorodnosti poljarizacionno-opticheskih izobrazhenij defektov struktury monokristallov, osnovannoe na vejvlet-analize” (“Removing of background inhomogeneity of polarize-optical images of structure defects in monocrystals, based on the wavelet analysis”, in Russian), Investigated in Russia, 142, 1434-1441 (2005)

27. G. W. H. Wurpel, H. A. Rinia, and M. Müller, “Imaging orientational order and lipid density in multilamellar vesicles with multiplex CARS microscopy”, J. Microsc. 218, 37-45 (2005).

28. G. W. H. Wurpel and M. Müller, “Water confined by lipid bilayers: A multiplex CARS study,” Chem. Phys. Lett. 425, 336-341 (2006)

29. H. Kano, H. Hamaguchi, “VIbrationally resonant imaging of a single living cell by supercontinuum-based multiplex coherent anti-Stokes Raman scattering microspectroscopy,” Opt. Express, 13, 1322-1327 (2005).

30. E. O. Potma, X. S. Xie, L. Muntean, J. Preusser, D. Jones, J. Ye, S. R. Leone, W. D. Hinsberg, and W. Schade, “Chemical imaging of photoresists with coherent anti-Stokes Raman scattering (CARS) microscopy”, J. Phys. Chem. B 108, 1296-1301 (2004).

31. M. Y. Vallah, V. V. Strelchuk, G. N. Semenova, Y. G. Savofiev, “Resonant Stokes and an anti-Stokes Raman scattering in nanostructures CdSe/ZnSe”, Solid state physics, vol. 46, no.1, 174-176 (2004)